



# Lab on a Chip

## Electrochemical Paper-Based Devices: Sensing Approaches and Progress Toward Practical Applications

Journal:	<i>Lab on a Chip</i>
Manuscript ID	LC-CRV-09-2019-000903.R1
Article Type:	Critical Review
Date Submitted by the Author:	08-Oct-2019
Complete List of Authors:	Noviana, Eka; Colorado State University, Chemistry McCord, Cynthia; Colorado State University, Chemistry Clark, Kaylee; Colorado State University, Chemistry Jang, Ilhoon; Colorado State University, Chemistry Henry, Charles; Colorado State University, Chemistry;

SCHOLARONE™  
Manuscripts

## **Electrochemical Paper-Based Devices: Sensing Approaches and Progress Toward Practical Applications**

Eka Noviana<sup>a,b</sup>, Cynthia P. McCord<sup>a</sup>, Kaylee M. Clark<sup>a</sup>, Ilhoon Jang<sup>a,c</sup> and Charles S. Henry<sup>a,\*</sup>

<sup>a</sup>Department of Chemistry, Colorado State University, Fort Collins, CO, USA

<sup>b</sup>Department of Pharmaceutical Chemistry, School of Pharmacy, Universitas Gadjah Mada, Yogyakarta, Indonesia

<sup>c</sup>Institute of Nano Science and Technology, Hanyang University, Seoul, South Korea

\*Corresponding author: [Chuck.Henry@colostate.edu](mailto:Chuck.Henry@colostate.edu)

### **Abstract**

Paper-based sensors offer an affordable yet powerful platform for field and point-of-care (POC) testing due to their self-pumping ability and utility for many different analytical measurements. When combined with electrochemical detection using small and portable electronics, sensitivity and selectivity of the paper devices can be improved over naked eye detection without sacrificing portability. Herein, we review how the field of electrochemical paper-based analytical devices (ePADs) has grown since it was introduced a decade ago. We start by reviewing fabrication methods relevant to ePADs with more focus given to the electrode fabrication, which is fundamental for electrochemical sensing. Multiple sensing approaches applicable to ePADs are then discussed and evaluated to present applicability, advantages and challenges associated with each approach. Recent applications of ePADs in the fields of clinical diagnostics, environmental testing, and food analysis are also presented. Finally, we discuss how the current ePAD technologies have progressed to meet the analytical and practical specifications required for field and/or POC applications, as well as challenges and outlook.

## 1. Introduction

The use of paper as a substrate for analytical measurements has been well known for over a century. Litmus paper and paper chromatography were invented in the early 1800s and 1900s, respectively, and are still common in analytical labs.<sup>1,2</sup> Paper-based dipstick and lateral flow assays have been used extensively for laboratory and point-of-care (POC) applications for decades.<sup>3</sup> More recently, the utilization of paper as an alternative to traditional microfluidics and its potential for diagnostic applications was demonstrated by Whitesides' group and has garnered significant interest from the analytical community.<sup>4</sup> The major difference between paper used for prior analytical devices and microfluidic paper-based analytical devices is the use of patterning methods to define flow. The interest in paper for analytical applications lies in its inherent characteristics of low cost, thin, lightweight, flexible, compatible with a wide array of patterning methods, easily disposable, versatile for modification with a variety of functional groups for performing analyte detection, and generation of flow without external pumps. Significant growth of academic research on paper-based analytical tools has been seen for the past decade with the aim of exploring the capability of this platform to perform analytical testing that is routinely carried out using bench-top instruments.<sup>5,6</sup>

While the majority of paper-based analytical technologies rely on colorimetric detection due to its ease of use and seemingly simple data interpretation, this mode of detection often suffers from limited sensitivity, small linear ranges and/or high detection limits. Color formation on paper substrate may reach saturation, colorimetric reactions are often hard to detect at low concentrations, and some sample matrices could provide background color on the paper.<sup>7</sup> The Henry group proposed electrochemical detection on paper devices in 2009 as an alternative to the colorimetric detection.<sup>8</sup> High sensitivity and selectivity can be easily achieved in electrochemical paper-based analytical devices (ePADs) through selection of electrode material, electrochemical technique, electrode potential, and/or coupling with recognition elements to the analyte, enzymes, nanoparticles, etc.<sup>9</sup> In addition, electrochemical measurements can be done relatively fast (seconds to minutes), which is particularly useful when dealing with a large number of samples and/or at the point-of-need. Significant trends in research on ePADs include studies on

electrode fabrication, electrochemistry on the electrodes on paper, strategies to improve analyte detection and potential applications of ePADs. This review aims to present critical perspective on those notable milestones while focusing on more recent progress for improving electrochemical sensing in paper devices and bringing the technology closer to practical applications. An excellent review on device consideration for development of ePADs was published by the Kubota group<sup>10</sup> and complements our review with more extensive elaboration on the device fabrication including selection of paper.

## 2. Fabrication of Paper Devices

While not obvious, paper is a logical material for producing analytical devices. Important advantages of the paper substrate include its accessibility, affordability, and ease of disposal compared to traditional materials used in microfluidics. In addition, many techniques exist for processing paper. These techniques allow printing, coating, cutting and lamination of paper for the production of point-of-care (POC) devices, resulting in mass producible products with low-cost.<sup>11</sup> Another important advantage of paper as a substrate is its porous, hydrophilic structure. Cellulosic paper can drive fluid flow without an external pump through capillary force. In addition, the cellulosic structure makes it possible to change properties of paper such as hydrophobicity, conductivity, and reactivity by modifying the chemical structure.<sup>5</sup> However, the basic performance of the paper-based device is significantly dependent on the paper properties including porosity, pore size, thickness, and type of material.<sup>12</sup> Therefore, the proper paper should be selected to fit the specific application.

Fabrication of a hydrophobic barrier is a common method to define flow channels in paper devices. This fabrication concept for paper channels was first introduced by Muller et al in 1949<sup>13</sup> and has been attracting attention since the first microfluidic paper-based analytical device ( $\mu$ PAD) fabricated using photolithography was introduced in 2007.<sup>4</sup> Photolithography uses a chemical photoresist absorbed into the paper substrate to generate the barrier by exposing the system to light through a photomask. Although photolithography has good resolution, it suffers from the high cost of organic solvents and photoresist, the brittle nature of the resulting devices, and the potential for the paper to generate background signals.<sup>14</sup> Other printing techniques have become more popular for fabricating paper-based devices to simplify the fabrication process and reduce costs. Hydrophobic barriers have been printed using

wax, indelible ink, ultraviolet-curable ink, and alkyl/alkenyl ketene dimer (AKD).<sup>11</sup> In recent ePAD studies, wax has been the most commonly used barrier material. Several printing techniques have been used to define flow channels and sample wells with wax. Among them, wax printing<sup>15</sup> using a commercial wax printer to print wax on a paper substrate, followed by heating to allow the wax to permeate the paper, is the most frequently used method to fabricate channels due to its simplicity.<sup>16-28</sup> Screen printing, which was first utilized to make a wax pattern of the channel boundary in 2011,<sup>14</sup> is a simple alternative to print hydrophobic materials on a paper substrate. Oliveira et al. used a dipping method with a wax-transfer mask by cutting the low tack transfer tape attached to the paper and dipped it into molten wax.<sup>29</sup> Qin et al. dipped half of carbon nanotube (CNT) paper strip into melted wax to cover and insulate paper device.<sup>30</sup> Another approach used a mixture of polydimethylsiloxane (PDMS) and curing agent tetraethyl orthosilicate (TEOS) printed on the paper using screen printing.<sup>31</sup> Inkjet printing has been used by Amatatongchai et al.<sup>32</sup> to create AKD barriers. Finally, black permanent ink was used for patterning the hydrophobic barriers by installing into the plotter.<sup>33</sup>

Another fabrication method cuts paper to directly form flow channels.<sup>34</sup> Unlike the hydrophobic barrier methods, cutting does not require materials to change chemical properties of the paper and can be used with widely available equipment such as scissors. Fava et al.<sup>35</sup> and Cincotto et al.<sup>36</sup> used a simple cutter printer to cut microfluidic patterns of 16 channels circularly distributed around the injection point and the microfluidic pathway, respectively. A laser cutter has also been used to create paper devices from Whatman SG81 and 3MM filter paper by Primpray et al.<sup>37</sup> and Gomez et al.<sup>38</sup>

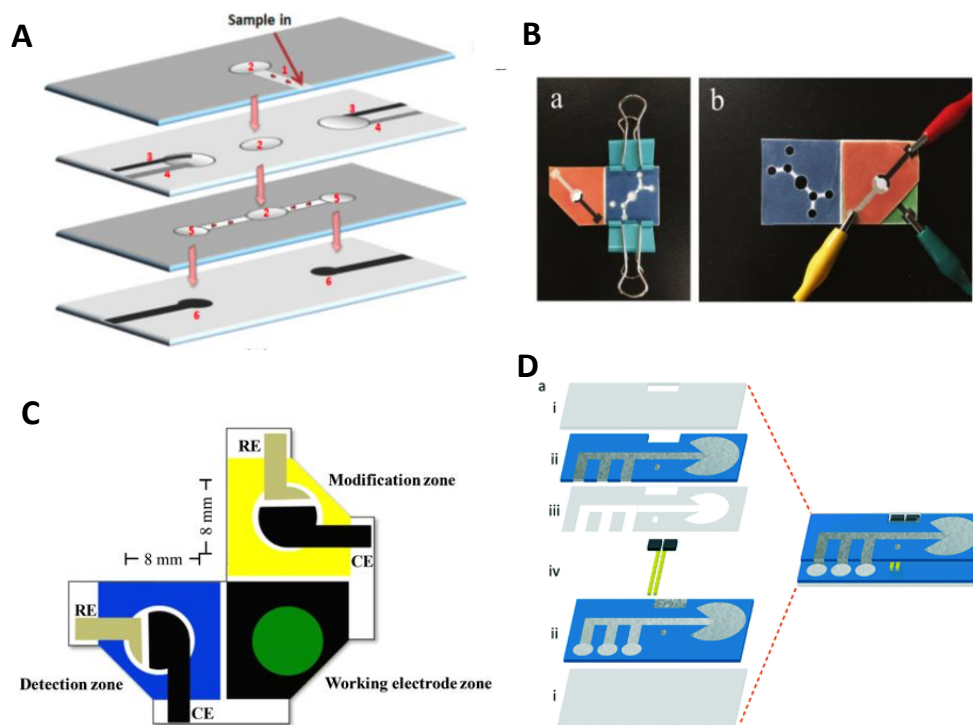


**Fig. 1** Multi-layered ePADs for improving device performance: (A) Schematic illustration of a multi-layered device fabricated using lamination. Reprinted with permission from ref<sup>39</sup>: Y. Wang, J. Luo, J. Liu, X. Li, Z. Kong, H. Jin and X. Cai, *Biosens. Bioelectron.*, 2018, **107**, 47-53 (Copyright 2018 Elsevier). Implementation of (B) multi-detection mode and (C) multi-step assay in a single device by utilizing origami method. Reprinted with permission from ref<sup>40</sup>: X. Sun, H. Wang, Y. Jian, F. Lan, L. Zhang, H. Liu, S. Ge and J. Yu, *Biosens. Bioelectron.*, 2018, **105**, 218-225 (Copyright 2018 Elsevier) and ref<sup>41</sup>: K. Pungjunun, S. Chaiyo, I. Jantrahong, S. Nantaphol, W. Siangproh and O. Chailapakul, *Microchim. Acta*, 2018, **185**:324 (Copyright Springer-Verlag GmbH Austria, part of Springer Nature 2018). (D) Fast flow channel consisting of a gap and electrodes. Reprinted with permission from ref<sup>42</sup>: R. B. Channon, M. P. Nguyen, A. G. Scorzelli, E. M. Henry, J. Volckens, D. S. Dandy and C. S. Henry, *Lab Chip*, 2018, **18**, 793-802 (Copyright 2018 Royal Society of Chemistry).

Once the basic fabrication of the paper-based channel is established, various methods can be used to improve channel performance such as multiplexed and sequential detection, flow rate control and on/off switching. As mentioned earlier, paper is porous and fluid flow within the paper is dominated by capillary forces.<sup>43</sup> Therefore, even if the top and bottom of the channel are uncovered, the fluid does not leak and stays in the channel until another paper layer or absorbent material is placed in contact. Using this characteristic, vertical flow has been achieved by lamination using paper and tape.<sup>44</sup> Combined horizontal and vertical flows have been utilized for multiplexed detection. Wang et al. fabricated a multi-layered device consisting of the inlet, electrode, and flow channel layers. In this device, sample fluid flows through a horizontal channel into two detection zones (Fig. 1A).<sup>39, 45</sup> Origami can

also be easily applied to paper-based devices due to the flexibility of paper substrate. This method makes it easy to stack multiple layers of paper by folding. Paper channels with multiple flow functions have been fabricated side-by-side on a single paper layer and then assembled using origami methods.<sup>46-48</sup> Connecting the sample area to the electrode by folding the paper has also been used as a start trigger for analysis.<sup>49-52</sup> Another advantage of the origami method is that multiple detection methods can be implemented in a single device. Dual-mode colorimetric and electrochemiluminescent detection of  $\text{Pb}^{2+}$  has been implemented in an origami device.<sup>53</sup> A similar strategy was implemented by Sun et al. who combined colorimetric and electrochemical detection (Fig. 1B).<sup>40</sup> Pungjunun et al. integrated both steps of electrodeposition and detection by fabricating three zones on a single paper layer (Fig. 1C).<sup>41</sup> Wang et al. fabricated a dual-mode cytosensor for the detection of MCF-7 cancer cells.<sup>54</sup> Finally, Arduini et al. developed an analytical device that can make several measurements for both initial and residual enzymatic activity estimation using origami geometry.<sup>55</sup>

Flow rate is an important aspect in sensing within ePADs. Controlling flow rates can decrease analysis time and provide sequential flow of various reagents. However, it is often difficult to manipulate flow rate in paper because the capillary force (which depends on the type of fluid and paper) is the only fluid driving force on the paper-based device. Initial flow control studies adjusted the flow rate by changing the hydrophobicity and using smaller pore size paper substrates.<sup>56</sup> New research on controlling flow rate in paper utilizes the concept of a hollow channel that consists of paper on at least one side and another substrate, sometimes paper, on the other. This kind of paper-based channel still employs a capillary force to drive fluid and has a gap connected with a porous area to increase the overall rate of the flow. The hollow channel is fabricated by combinations of paper, glass slide, transparency film, double-sided adhesive, and more.<sup>42, 56</sup> Recent studies have shown that paper-based channel with a gap (Fig. 1D) can produce much faster flow than a typical paper-based channel, resulting in a short total analysis time<sup>42</sup> and can be used to incorporate the electrode arrays into the gap flow to improve sensing performance.<sup>57</sup>

### 3. Fabrication of Electrodes

Electrode fabrication is a crucial step in the fabrication of an effective ePAD. The first reported ePAD from the Henry group in 2009 screen-printed carbon electrodes onto filter paper.<sup>8</sup> Since then, various other electrode fabrication techniques have been presented in the literature such as stencil printing,<sup>17, 29, 36, 58, 59</sup> inkjet printing,<sup>60-65</sup> microwire placement,<sup>42, 66</sup> laser scribing,<sup>67</sup> using carbon tape,<sup>38</sup> pencil drawn,<sup>68, 69</sup> spray and spin coating,<sup>70</sup> and sputtering.<sup>28, 71, 72</sup>

### 3.1. Screen-printed electrodes

Screen-printed electrodes (SPEs) were the first electrodes incorporated into an ePAD and have since become the most popular electrode fabrication technique for ePADs.<sup>8, 46, 51, 55, 73-76</sup> Screen printing is a simple electrode fabrication technique where specially made screens or meshes, typically made from silk or nylon, are used to print electrodes into patterns defined by the screens. These meshes are designed with computer software and created through an emulsion process resulting in a negative cut out of the desired electrode geometries. Conductive ink is spread onto these screens after they have been placed on the substrate. Most inks are thermally cured at 60-90 °C for several minutes after printing. Often these electrodes involve multiple applications of different inks and meshes that must be aligned (e.g. one ink for the working and counter electrodes and one for the reference electrode). Screen printing equipment is fairly inexpensive and many systems perform these steps automatically.<sup>77</sup> Due to low cost and ease of fabrication, screen-printing allows for convenient incorporation in ePADs. For example, SPEs have been incorporated into complex designs like 3D origami devices.<sup>46, 55</sup> Screen-printing can also easily be scaled up for mass production, and SPEs fabricated with screen printing machinery tend to be reproducible since the fabrication is automated.

Screen-printing not only allows for easy fabrication but also simple modification of electrodes using different conductive inks. The ability to add catalysts to the ink adds versatility without complicated post-modification steps. There are numerous commercially available carbon and metallic inks that can be used with screen printing equipment, and many groups prepare their own inks.<sup>76</sup> Carbon inks have become a popular choice in electrode fabrication for working and counter electrodes in ePADs due to their low cost and availability. Carbon-based electrodes have wide potential windows and are less prone to fouling than precious metals which allows them to be used to detect a wide variety of analytes.<sup>78</sup> The most common reference electrode used is Ag/AgCl ink due to its

low-cost, low toxicity, and stable reference potential.<sup>8</sup> Many SPEs use a pseudo-reference electrode such as carbon or silver, where a thermodynamic equilibrium is not maintained and the reference potential can drift based on solution conditions.<sup>69</sup> Recently to provide better detection, SPEs have been modified for specific applications by using inks such as carbon black/Prussian blue nanocomposite-modified graphite ink,<sup>51</sup> graphene-modified carbon ink,<sup>74</sup> Co(II)phthalocyanine-modified carbon ink,<sup>75</sup> and Au nanoparticle ink.<sup>76</sup> Even with such modifications, the electrochemical properties of SPEs are unfortunately not as good as traditional metallic and conductive carbon electrodes with regards to electron transfer kinetics and electrode resistance.

### 3.2. Stencil-printed electrodes

Stencil printing is similar to screen printing but avoids the issue of requiring specialized screen making machinery. Instead, the electrode shapes for stencil printed electrodes can be cut into an open mask or stencil made from a material such as transparency sheets. The ink can then be spread over the stencil onto a piece of paper and smoothed using a squeegee, filling the exposed area on the paper as shown in Fig. 2A. Stencil-printed electrodes can be fabricated with various types of inks and related SPE inks. However, to ensure clean boundaries are obtained on the electrodes, it is often necessary for the ink to be more viscous, which can be achieved by altering the solvent ratio in the ink.<sup>58</sup>

An effective example of a stencil material that has been used in ePADs is low tack transfer tape (LTT). The electrode pattern is cut into the LTT using a craft cutter and then placed on the filter paper of the ePAD.<sup>29</sup> Other publications have used polyester stencils<sup>58</sup> or cut the masks out of transparency sheets using a commercial laser cutter.<sup>17, 36, 59</sup> Most stencil-printed electrodes employ traditional carbon paste materials using graphite; however, a stencil-printed boron-doped diamond (BDD) electrode was reported for the first time in ePADs recently.<sup>59</sup> The stencil-printed BDD electrodes demonstrated an improvement in background current, resistance to fouling, and detection limits without compromising the ease of fabrication.

Current methods for stencil printing electrodes are among the most cost effective due to the lack of equipment and use of inexpensive materials. Lack of uniformity in this technique is a major obstacle since they are fabricated by hand; however, this concern could be eliminated when the fabrication is automated for mass production. Both

screen and stencil printing require an excess of conductive ink to make the electrodes and therefore have a relatively significant amount of waste associated with the fabrication.

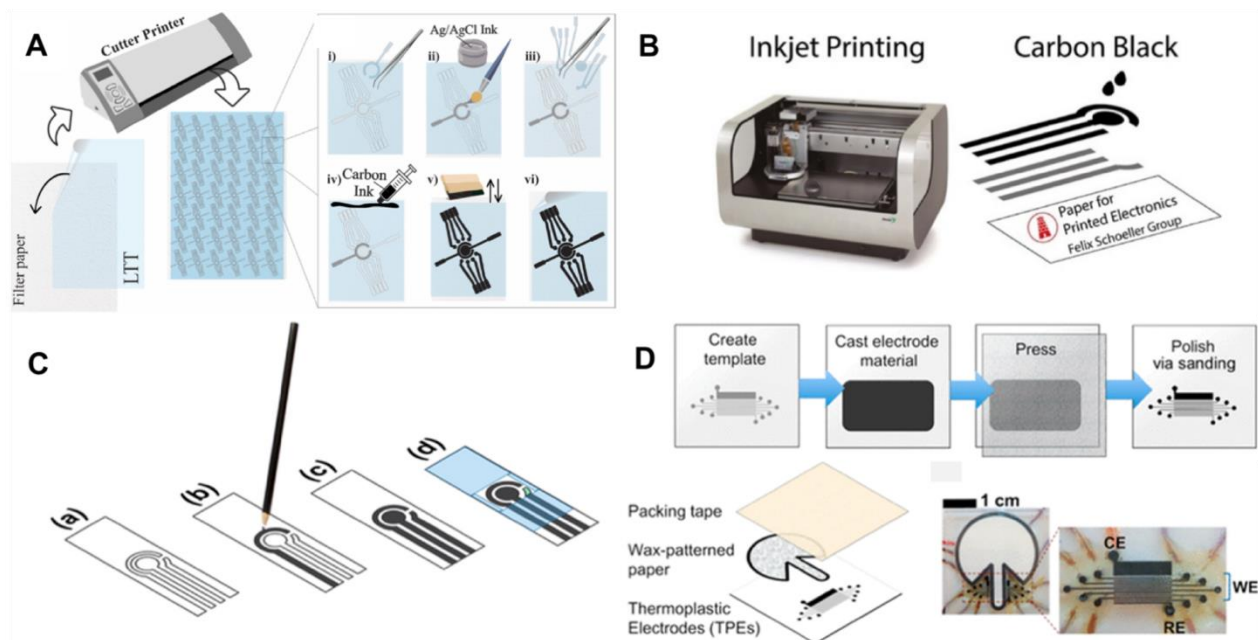


**Fig. 2** Electrode fabrication schemes for: (A) Stencil-printed electrodes. Adapted with permission from ref<sup>29</sup>: C. Kokkinos, A. Economou and D. Giokas, *Sens. Actuators B: Chem.*, 2018, **260**, 223-226 (Copyright 2019 Elsevier). (B) Inkjet-printed electrodes. Adapted with permission from ref<sup>60</sup>: S. Cinti, N. Colozza, I. Cacciotti, D. Moscone, M. Polomoshnov, E. Sowade, R. R. Baumann and F. Arduini, *Sens. Actuators B: Chem.*, 2018, **265**, 155-160 (Copyright 2018 Elsevier). (C) Pencil-drawn electrodes. Adapted with permission from ref<sup>68</sup>: F. J. Gomez, P. A. Reed, D. G. Casamachin, J. R. de la Rosa, G. Chumanov, M. F. Silva and C. D. Garcia, *Anal. Methods*, 2018, **10**, 4020-4027 (Copyright 2018 Wiley). (D) Thermoplastic electrodes. Adapted with permission from ref<sup>57</sup>: E. Noviana, K. J. Klunder, R. B. Channon and C. S. Henry, *Anal. Chem.*, 2019, **91**, 2431-2438 (Copyright 2019 American Chemical Society).

### 3.3. Inkjet-Printed Electrodes

Inkjet printing electrodes is becoming increasingly popular. In inkjet printing, the conductive ink is printed onto the substrate with a commercial inkjet printer in the desired pattern (Fig. 2B). The only difference between being able to inkjet print an electrode and an ordinary document is that the printer cartridge is filled with conductive ink to be used as the electrode material. Inkjet-printed electrodes have been fabricated with a variety of conductive inks including carbon,<sup>60</sup> multiwall carbon nanotubes,<sup>64</sup> Ag nanoparticles,<sup>60</sup> and graphene nanopowder inks.<sup>62</sup> These inks must have low viscosity relative to other electrode printing techniques to prevent clogging the printing system.<sup>60</sup> An advantage of inkjet-printed electrodes is that electrode thickness can be tuned by printing multiple layers to

lower resistance and improve robustness.<sup>64</sup> Ruecha et. al. reported the fabrication of a single-use ePAD for ion sensing solely using an inkjet printer. This type of electrode often involves multiple tedious modification steps when done separately. However, by using an inkjet printer with multiple nozzles and cartridges, the authors were able to eliminate the hassle. The authors printed wax barriers for the channels, FeCl<sub>3</sub>, a reference membrane, KCl, graphene ink, and an ion selective membrane onto the ePAD with precision as shown in Fig. 3.<sup>62</sup> This work demonstrates the possibility of fabricating low cost sensors for complicated detection schemes.

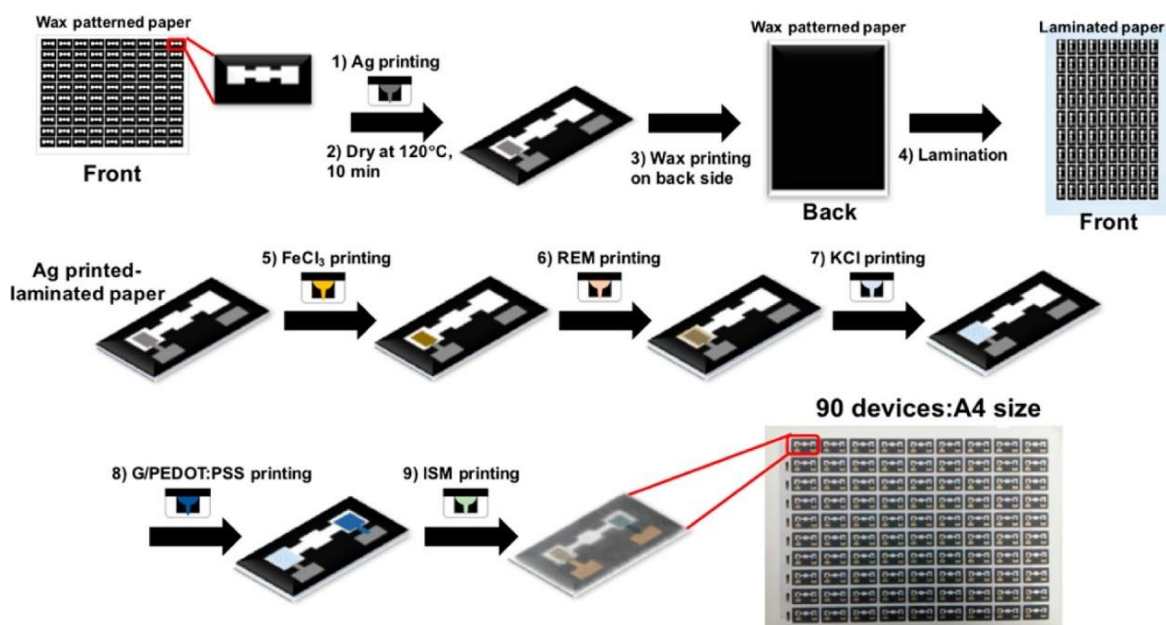


**Fig. 3** All-in-one electrode fabrication and modification scheme for ion sensing done solely with inkjet printer. Adapted with permission from: ref<sup>62</sup>: N. Ruecha, O. Chailapakul, K. Suzuki and D. Citterio, *Anal. Chem.*, 2017, **89**, 10608-10616 (Copyright 2017 American Chemical Society).

The potential for an all-in-one fabrication method is a major advantage for inkjet printing electrodes. This technique, unlike other popular techniques, does not require construction of a mask or screen prior to fabrication, saving both time and money. Inkjet printing also eliminates some of the waste involved in screen and stencil printing and provides better resolution, which may become important for intricate patterning. Due to the already automated nature of this technique and reduced waste, inkjet printing electrodes would be able to move to large-scale

production efficiently. As the field continues to expand, it is likely that inkjet printing will be able to replace tedious modification steps for complex devices.

### 3.4. Pencil/pen-drawn electrodes

Dossi et. al. first introduced free hand pencil-drawn electrodes using a commercially available graphite pencil to draw working and counter electrodes.<sup>79</sup> Several other groups subsequently reported using manually drawn pencil graphite electrodes.<sup>68, 69</sup> To make the electrodes more consistent, toner lines or stencils have been employed to delimit the electrode area to produce traditional three electrode systems in ePADs as shown in Fig. 2C.<sup>68, 69</sup> One advantage of this technique is that since the graphite is transferred directly to the paper, no additional binder is necessary, and no waste is produced like in screen- and stencil-printing. Unlike other fabrication techniques, no thermal curing is required. Without a binder, however, the thickness of the electrode cannot be easily controlled, thus potentially affecting electrode conductivity.

Pen drawing is a similar technique that uses inexpensive materials to draw electrodes directly onto a piece of paper by hand. Ballpoint pens are modified to dispense carbon inks. Li et al. reported a hand-drawn fabrication of ePADs using a carbon ink-modified ballpoint pen for rapid prototyping.<sup>80</sup> The electrodes were written directly onto the filter paper using a ruler as the guide. After curing in the oven at 70°C for 30 min, wax channels were drawn around the electrodes with a heated modified pen containing the wax.<sup>80</sup> An obstacle for both pencil- and pen-drawn electrodes is the difficulty to produce consistent electrodes because differences in pressure greatly impact the deposition of the electrode material onto the paper. These techniques will be difficult to scale up for mass production, but they should be useful for research and prototyping.<sup>80</sup>

### 3.5. Microwire Electrodes

Microwires as electrodes in ePADs were first proposed by Fosdick et al. where Au microwires were cleaned and attached to the ePAD with Cu tape and Ag paint.<sup>81</sup> Incorporating microwires into ePADs is a fabrication technique that allows more flexibility in the electrode material. Adkins et al. compared stencil-printed carbon electrodes in ePADs to several types of microwires in ePADs (Au, Pt, Pd, Pt with 8% W, and Pt with 20% Ir).<sup>82</sup> Results showed that all electrodes gave reasonable responses in the presence of  $\text{Fe}(\text{CN})_6^{3-/4-}$ , and the electrochemical performance of the microwires were superior to the stencil-printed electrodes.<sup>82</sup> The improved performance of

microwires is a result of lower resistance and higher electroactive surface area than carbon composite electrodes. In the past couple years, there have only been a few reports using microwires in ePADs. One report incorporated Au microwires modified with antibodies to capture and detect virus particles through a stepwise bioconjugation process.<sup>66</sup> Another device incorporated Au microwires into a fast flow ePAD for detection of Cd with stripping voltammetry.<sup>42</sup>

Researchers may be discouraged from using microwires in ePADs, as they are fragile and difficult to handle. Precious metal microwires also raise the cost of the ePAD. However, there are many advantages that should be noted. Microwires can be cleaned and modified before the electrodes are added to the ePADs, which prevents the modification and cleaning steps from damaging or contaminating other parts of the ePAD. Microwires also do not have some of the drawbacks of carbon composite electrodes such as poor electrochemical properties and electrode irreproducibility.

### **3.6. Other fabrication techniques**

Recent publications have demonstrated several other less common yet noteworthy electrode fabrication techniques. One example is fabricating electrodes by sputtering metals on paper. Sputtering requires a vacuum and specialized sputtering chamber, which limits the applications due to the costly equipment. For ePADs, a mask is placed over the paper to define the electrode region,<sup>72</sup> and metal can be sputtered multiple times to control the thickness of the metal film.<sup>28</sup> Recent works reported the use of Pt,<sup>28, 71</sup> Ag,<sup>28</sup> Sn,<sup>28</sup> and Au-sputtered working electrodes.<sup>72</sup> While this technique provides high performance electrodes, scaling up the fabrication for mass production is unlikely due to the expensive equipment and materials involved. A main incentive for using ePADs is the cost-effectiveness. Therefore, sputtering may be an excellent tool for laboratory studies but limited for commercial applications.

Pyrolyzed carbon electrodes from paper were first introduced by Giuliani et al. fabricated using a tube furnace.<sup>83</sup> A recent report by de Araujo et al. demonstrated laser scribing electrodes to accomplish pyrolysis with less extreme conditions.<sup>67</sup> This technique radiates paperboard with a CO<sub>2</sub> laser to pyrolyze the carbon directly onto the paperboard surface.<sup>67</sup> The patterned pyrolyzed carbon surface was used as the working and counter electrode, while Ag paint was applied for the reference. Laser scribing is reagent-less and can be easily integrated into ePADs at

low cost.<sup>67</sup> Laser-scribed electrodes have the potential to become a more popular electrode fabrication technique in ePADs and be easily scaled up for mass production.

Another approach to incorporating electrodes into paper-based devices is making the electrode off-chip. Having the electrode separate from the paper portion of the ePAD allows the electrode to be removed and reused for another device while the paper portion is disposable. Off-chip electrodes also allow for the electrodes to be polished between uses. Santhiago et al. reported an off-chip electrode attached with double sided tape.<sup>84</sup> In this work, a capillary tube was filled with pencil graphite and sealed with epoxy. By having an off-chip electrode, the extra space on the ePAD could be utilize for interesting features like a quick response (QR) code to give the device user rapid results.<sup>84</sup> Thermoplastic electrodes (TPEs) are another example of off-chip electrodes in ePADs reported by Noviana et al.<sup>57</sup> In this work, TPEs were fabricated by mixing graphite in solvated cyclic olefin copolymer and heat-pressed into an acrylic template as shown in Fig. 2D. The TPEs were patterned into an interdigitated electrode array (IDA) with eight working electrodes, where the electrodes alternate oxidizing and reducing the analyte to enhance the cumulative signal.<sup>57</sup> TPEs have shown improved electrochemical activity over traditional carbon composite electrodes like SPEs and comparable to that of conventional glassy carbon and Pt electrodes.<sup>85</sup> Very few publications have shown the use of electrode array systems in ePADs as opposed to the primarily used three electrode system.<sup>86, 87</sup> With off-chip electrodes, advanced electrode schemes in ePADs has been shown to be a feasible option and should be further explored. This approach could inspire the incorporation of many other composite materials previously studied such as Teflon,<sup>88</sup> epoxy,<sup>89</sup> as well as new composites yet to be published.

## 4. Sensing motifs

### 4.1. Direct detection

Direct detection is the simplest detection motif where the measured electrochemical signal comes from the analyte of interest instead of a label, product, or mediator. Direct detection with chronoamperometry and various voltammetry techniques can be used for determination of redox active species.<sup>18, 28, 41, 68, 90-93</sup> Direct detection is frequently utilized for metals,<sup>18, 28, 41</sup> redox active small biomolecules,<sup>36</sup> and redox active drug analytes.<sup>68, 90</sup> For direct detection, catalysts and other detection enhancements such as nanomaterials can be easily mixed into or

deposited onto electrode materials.<sup>36, 41, 92-96</sup> These electrode materials are cheap, easy to make, and disposable which can eliminate electrode fouling concerns by allowing them to be single use.<sup>91</sup>

For direct detection of metals, anodic stripping voltammetry (ASV) is commonly used to preconcentrate the analytes at the electrode surface by holding the electrode at a negative potential prior to sweeping the potential towards oxidative potentials.<sup>18, 28, 41</sup> An early report by Nie et al. utilized a paper channel with a cellulose waste pad to generate flow over the working electrode to aid in deposition of metals on the electrode surface. Flow over the working electrode increased sensitivity for Pb(II) by a factor of five over stagnant detection.<sup>94</sup> Utilizing paper to generate flow over electrodes is also advantageous for reducing adsorption of bubbles and contaminants. Filter paper strips placed onto SPEs has been used to generate flow for enhanced simultaneous detection of Pb(II) and Cd(II).<sup>95</sup> Bismuth is often co-deposited with target metals onto carbon electrodes to enhance detection with ASV.<sup>94-97</sup> Along with bismuth enhancement, Tan et al. used paper to pre-store Zn(II) as an internal standard for detection of Pb(II).<sup>97</sup> Metal detection can also be enhanced through the properties and structure of the base electrode material. Recently, Kokkinos et al. developed a multiplexed ePAD for determination of Zn(II) and Pb(II) with square wave anodic stripping voltammetry (SW ASV) on sputtered Sn film electrodes (Fig. 4).<sup>28</sup> The rough surface of the sputtered film on the paper substrate provided a large active surface area, resulting in approximately 1 µg/L (1 ppb) detection limits for each species without further electrode modification.<sup>28</sup> To determine the total concentration of a specific metal when multiple oxidation states are present, a reducing agent can be added. For example, a recent ePAD reported by Pungjunun et al. used thiosulfate to reduce As(V) to As(III) prior to performing SW ASV for total arsenic determination.<sup>41</sup> Using paper as a substrate can simplify the assay by creating a multi-step paper-based analytical device where deposition, reduction, and oxidation steps can be performed within the same device through origami folding.<sup>41</sup> Linear sweep voltammetry (LSV) has also been combined with ASV as an electronically simpler technique for direct determination of Hg(II) in environmental water samples.<sup>18</sup>

Other analytes detected directly with ePADs are organic molecules related to diagnostic,<sup>19, 90, 98</sup> food safety<sup>29</sup> and forensic applications.<sup>68, 93</sup> For organic analytes, electrode fouling can be a major concern. Therefore, the disposable nature of ePADs is a major benefit. Some of these analytes are measured with the amperometry.<sup>19</sup> Pulsed voltammetry methods such as differential pulse voltammetry (DPV) and square wave voltammetry (SWV) are also

commonly used in applications requiring low detection limits because of their ability to subtract non-faradaic current.<sup>29, 68, 90, 98</sup> For multiplexed analysis of redox active analytes occurring at similar potentials, surfactants, nanocomposites and amino acids can be added to the working electrode to help separate peaks.<sup>91</sup> A recent report utilized Au-coated Fe<sub>3</sub>O<sub>4</sub> nanoparticles modified with cysteine and polyaniline (Fe<sub>3</sub>O<sub>4</sub>@Au-Cys/PANI) for the simultaneous determination of ascorbic acid, dopamine, and uric acid.<sup>91</sup> The composite improved electrocatalytic oxidation of the three species and when combined with sodium dodecyl sulfate (SDS) surfactant allowed the three peaks to be resolved with DPV.<sup>91</sup>

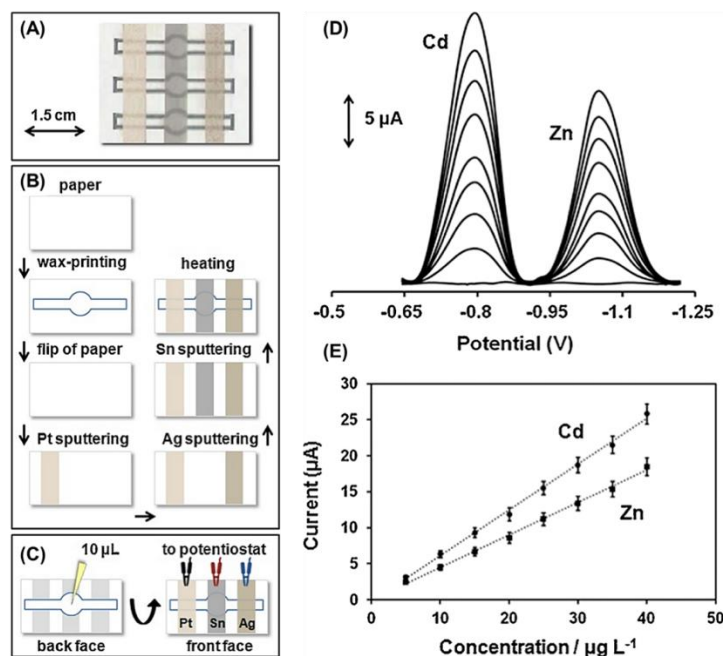


**Fig. 4** Sputtered Sn film ePAD for simultaneous Cd(II) and Zn(II) detection. (A) ePAD photograph, (B) ePAD fabrication schematic, (C) SW ASV of 0–40 µg/L Cd(II) and Zn(II), and (D) respective calibration curves. Reprinted with permission from ref<sup>28</sup>: C. Kokkinos, A. Economou and D. Giokas, *Sens. Actuators B: Chem.*, 2018, **260**, 223-226 (Copyright 2018 Elsevier)

For direct detection in ePADs, nanomaterials and catalysts are commonly used to modify carbon ink and carbon paste working electrodes for increased sensitivity and improved detection limits. Common nanomaterials used include nanoparticles<sup>41, 91, 92</sup> and various forms of graphene and graphene oxide.<sup>92</sup> The electrocatalytic properties of nanomaterials and catalysts can shift oxidation to lower potentials to aid in selectivity. The physiochemical properties of nanomaterials have also been of use to affect mass transport.<sup>36, 92</sup> For direct nitrite detection, the high surface area of graphene nanosheets and gold nanoparticles was utilized to create a thin diffusion layer to improve

sensitivity, resulting in superior performance relative to commercial electrodes.<sup>92</sup> Nanomaterials can also be used to aid detection through intermetallic binding. Au nanoparticle-modified electrodes for determination of arsenic created stable Au-As intermetallic bonds during deposition which can easily be oxidized for improved arsenic detection.<sup>41</sup> Zn oxide nanorods were used for 3,4-methylenedioxymethamphetamine (MDMA) detection in remote sensing diagnostic applications. Zn oxide nanorods are biocompatible and provide high surface area for fast electron transfer.<sup>93</sup> Nanomaterials and catalysts allow for direct detection of analytes traditionally detected with more complex detection modes. An ePAD for the detection of glucose was assisted by the catalyst Co(II)phthalocyanine, an ionic liquid, and graphene.<sup>19</sup> The improved ionic conductivity and hydrophilicity from the ionic liquid, and the increased surface area and conductivity of graphene allowed the glucose to be detected non-enzymatically with chronoamperometry.<sup>19</sup>

#### **4.2. Potentiometric detection**

Ion selective electrodes can be utilized as a simple detection motif for analytes that are not redox active through ionophore-based potentiometric sensing in paper-based devices.<sup>62, 99, 100</sup> Ion selective electrodes (ISEs) utilize an ionophore specific to the analyte of interest for selective potentiometric detection through ionophore-analyte interactions. In recent ePAD literature, ISEs have been used for detection of metal cations,<sup>62, 99, 101</sup> halide anions,<sup>99</sup> and diagnostic biomarkers.<sup>100</sup> A disposable paper-based ISE for bilirubin detection, a key indicator of liver health, was developed and capable of measuring clinically relevant bilirubin concentrations. All components of traditional ISEs were incorporated into the paper-based device including sample and reference solutions connected by a paper-based salt bridge.<sup>100</sup> A simplified solid contact paper-based ISE with a solid contact reference electrode was recently developed for multiplexed detection of Na<sup>+</sup>, K<sup>+</sup>, and I<sup>-</sup> ions with sub-micromolar detection limits.<sup>99</sup> For the ISEs, an ionophore cocktail was dropcast onto single walled carbon nanotube (SWCNT) electrode supports for specificity and the reference electrode was made of a copolymer (methyl methacrylate-co-decyl methacrylate) and ionic liquids for maintaining a stable potential.<sup>99</sup>

#### **4.3. Enzymatic detection**

Enzymatic detection utilizes enzyme activity to quantify an analyte of interest. The first report of an electrochemical paper-based device by Henry group in 2009 utilized glucose oxidase, lactate oxidase, and uricase

for multiplexed determination of glucose, lactate and uric acid.<sup>99</sup> This was achieved by spotting three different analyte specific enzyme solutions into separate detection zones within the electrochemical cells.<sup>8</sup> Enzyme detection can be based on quantifying enzyme activity<sup>102</sup> or enzyme inhibition<sup>6,103</sup> in the presence of the target. Enzymatic electrochemical detection is generally achieved through an electroactive enzymatic by-product or redox mediator. Most enzymatic ePADs use chronoamperometry detection to measure the electroactive species, which is proportional to the analyte, simply through current response.<sup>16, 51, 102, 104</sup> Pulsed methods such as differential pulse amperometry (DPA),<sup>21</sup> SWV,<sup>36</sup> and coulometry<sup>102</sup> have also been used to improve sensitivity and limits of detection. Paper-based devices allow for all reagents needed for enzymatic detection to be stored along paper microfluidic channels and redissolved upon sample introduction.<sup>51, 102</sup>

Enzyme immobilization on ePADs is simple because paper substrates allow adsorption of enzymes without denaturation through electrostatic interactions between the enzymes and the paper substrate.<sup>105</sup> Often in ePADs, enzymes are merely dropcast onto the device for physical adsorption in the detection zone or specifically the working electrode surface.<sup>8, 16, 21, 51, 104</sup> Enzymes can also be immobilized onto ePADs using glutaraldehyde crosslinker which readily forms stable links to various nucleophiles such as amines, thiols, and hydroxyl groups for stronger immobilization.<sup>36</sup> For potentiometric enzymatic sensing, enzymes have been immobilized through entrapment between two drop-casted membrane layers. Nafion membranes used to immobilize glucose oxidase for glucose detection resulted in increased sensitivity to enzymatic generation of electroactive by-product, H<sub>2</sub>O<sub>2</sub>, and minimized interference in the device.<sup>71</sup>

H<sub>2</sub>O<sub>2</sub>, thiocholine, and nicotinamide adenine dinucleotide (NADH) are common redox-active enzymatic by-products used to quantify various biologically relevant analytes. Nanoscale conductive carbon and Prussian blue nanocomposites are commonly used in enzymatic ePADs as electrocatalysts for detection of enzymatic by-products.<sup>30, 51, 102, 103, 106</sup> Prussian blue-carbon black<sup>7,102, 103</sup> and Prussian blue-carbon nanotube nanocomposites<sup>30</sup> have also been used to modify SPCEs. High surface area to volume ratios in nanoscale carbons act as favorable nucleation sites for Prussian blue.<sup>103</sup> These composites lower the oxidation potential and therefore reduce fouling comparatively to bare electrodes.<sup>102</sup> Various reductase enzymes have been employed with these nanocomposites in recent years for determination of analytes such as mustard gas (Fig. 5),<sup>51</sup> glucose,<sup>30</sup> paraoxon (a nerve agent

stimulant),<sup>103</sup> ethanol,<sup>106</sup> and butyrylcholinesterase.<sup>102</sup> Detection of NADH in ePADs is often enhanced with reduced graphene oxide.<sup>21, 104</sup> Electrochemically reduced graphene oxide can decrease the overpotential for NADH by providing edge plane active sites and increasing the active surface area and conductivity.<sup>21, 104</sup> Recent applications of enzymatic ePAD detection with NADH include neonatal screening of Phenylketonuria to diagnose problems with amino acid metabolism<sup>21</sup> and monitoring blood ketones, such as 3-hydroxybutyrate, for detection of life-threatening ketoacidosis.<sup>104</sup>

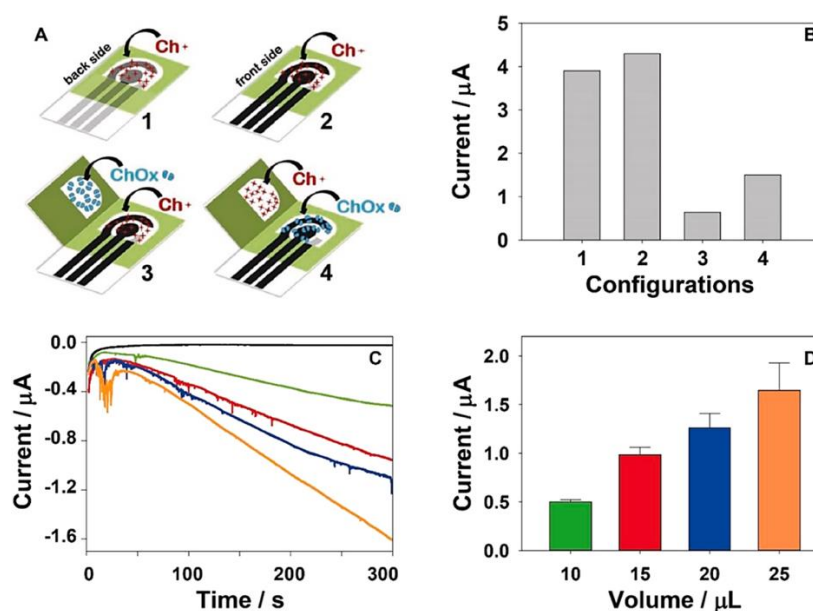


**Fig. 5** Choline oxidase (ChOx) enzymatic ePADs for mustard gas detection: (A) Schematics for four ePAD formats: one dimensional ePADs (where choline (Ch<sup>+</sup>) is pre-loaded onto the device) and origami devices where both Ch<sup>+</sup> and ChOx are preloaded onto the device, (B) H<sub>2</sub>O<sub>2</sub> amperometric response currents for the four formats, (C-D) Using origami-ePAD 4, amperograms and current intensity plot of the by-product H<sub>2</sub>O<sub>2</sub> when 5 µL (black), 10 µL (green), 15 µL (red), 20 µL (blue) and 25 µL (orange) of 50 mM phosphate buffer (pH 7.4) are added. Reprinted with permission from ref<sup>51</sup>: N. Colozza, K. Kehe, G. Dionisi, T. Popp, A. Tsoutsouloupoulos, D. Steinritz, D. Moscone and F. Arduini, *Biosens. Bioelectron.*, 2019, **129**, 15-23 (Copyright 2019 Elsevier)

Enzymatic detection can also be achieved using a redox mediator where electron transfer between the enzymatic reaction and a redox active molecule in the detection zone is used to quantify the analyte. Redox mediators used in ePADs in recent years include hexaammine-ruthenium(III) chloride<sup>36</sup> and ferrocyanide.<sup>16, 102, 107</sup> Hexaammine-ruthenium(III) chloride was used as a mediator for creatinine detection. Creatinine can be converted to creatine by creatininase inducing the oxidation of Ru(III) to Ru(II) which can be electrochemically determined with SWV.<sup>36</sup> With a cocktail of glucose oxidase (GOx), horseradish peroxidase (HRP), and ferricyanide, sensitive glucose

determination can be achieved through a cascade of reactions. The oxidation of glucose is catalyzed by GOx which generates  $H_2O_2$ . HRP then consumes the previously formed  $H_2O_2$  to catalyze the oxidation of ferrocyanide to ferricyanide which can be measured for amperometric determination of glucose.<sup>17,108</sup> Although enzymatic detection can be sensitive and selective, enzymes have issues related to temperature and pH sensitive stability.<sup>19, 109</sup> For these reasons, in recent ePAD literature, there has been a push toward non-enzymatic sensing of molecules traditionally sensed with enzymes through the utilization of nanomaterials for direct<sup>19, 26</sup> and indirect sensing.<sup>72, 109</sup>

#### 4.4. Affinity-based detection

Electrochemical affinity assays are based on biorecognition elements binding to a target to produce a change in electrochemical signal. The most common forms of these assays are antibody- or nucleic acid-based and allow detection of analytes that are not redox active. Recognition elements can be very sensitive to small changes in target levels and thus can provide very low detection limits (sub  $pg/mL$ <sup>48</sup> or 10 virus particles<sup>66</sup>). Immobilization of recognition elements on the working electrode surface is often a key component of electrochemical affinity assays in ePADs. The first step of most immobilizations is to terminate the electrode surface with functional groups that are easily conjugated to biorecognition elements through established crosslinker chemistries. Electrode surfaces can be modified with amine functional groups through electrodeposited PANI or by dropcasting chitosan polymers as examples.<sup>50, 74</sup> Electrodepositing conductive PANI also increases the electroactive surface area which aids immobilization and improves assay sensitivity.<sup>74</sup> The affinity between Au and thiols is often used to immobilize thiols terminated with carboxylic acids and other functional groups for further crosslinking. Thiol-terminated aptamer probes can also be used for direct adsorption to the electrode surface.<sup>45, 110</sup> Issues with thiol-Au stability in ePADs can be mitigated through multidentate thiols for added stability.<sup>66</sup>

Early reports in the field of paper-based electrochemical immunoassays utilized enzyme-linked immunosorbent assays (ELISAs), the most common type of immunoassay, where antibody-antigen binding is detected by an enzymatic label generating a redox active product.<sup>111</sup> To mitigate the problems associated with poor enzyme stability in ELISA assays, cyclodextrin functionalized AuNPs (CD@AuNPs) as well as Pt nanozymes have been used as reducing agents and enzyme mimic labels for antibodies.<sup>109, 112</sup> In a report by Yu et al., the binding of a Pt nanozyme-labeled antibody to immobilized carcinoembryonic antigen (CEA) on a carbon nanotube paper electrode

was used to quantify CEA through increased electrode resistance from nanozyme generated- $O_2$  pressure.<sup>37</sup> Label-free assays are becoming increasingly popular for ePAD immunoassays because they are less complex, require fewer steps, and have no stability issues stemming from an enzymatic label.<sup>66</sup> These assays frequently use electrochemical impedance spectroscopy (EIS) as it is highly sensitive to changes in electrode surface conditions.<sup>66</sup> Antibody-antigen binding at the electrode surface is quantified through the increase in charge transfer resistance of the surface to a redox mediator, commonly ferricyanide/ferrocyanide ( $[Fe(CN)_6]^{3-/4-}$ ).<sup>50, 74</sup> The increase in charge transfer resistance is usually correlated to antigen concentration by performing a full impedance spectra and measuring the change in diameter of the Nyquist plot semicircle.<sup>66, 74</sup> There is also interest in single frequency impedance assays because generating a full impedance spectrum is relatively time consuming (~2-5 min) compared to other electroanalytical techniques. For detection of C-reactive protein (CRP), an optimal frequency was found for antibody-antigen binding which was used to determine clinically relevant CRP concentrations without scanning a range of frequencies.<sup>50</sup> Quasi-steady state flow ePADs<sup>113</sup> have been utilized in label-free detection of West Nile virus on Au microwire electrodes.<sup>66</sup> Greater capture efficiency of the virus targets in flow lead to a wider linear range and lower detection limit. When the antigen is redox active, capture by antibody can act as a preconcentration step. For example, in a recent report by Scala-Benuzzi et al. a redox active pollutant, ethinyl estradiol (EE2), was captured on antibody modified paper micro-zones which were placed over a screen-printed electrode and desorbed with sulfuric acid for detection.<sup>114</sup>

Many ePAD immunoassays use nucleic acid recognition elements like aptamers and peptide nucleic acids (PNA). Nucleic acid probes can detect nucleic acid sequences through hybridization<sup>25, 115</sup> or through a binding induced structure change from a selective affinity for the target.<sup>45, 110</sup> Electrochemical detection with nucleic acids is typically performed by modifying the probe with a redox active label,<sup>115, 116</sup> incorporating a redox indicator into the electrode material,<sup>45, 110</sup> or measuring the resistance to charge transfer with impedance spectroscopy in the presence of the target.<sup>25, 117</sup> Nucleic acid probes have flexible structures, low cost, higher stability, and are more easily modified with specific functional groups for bioconjugation than antibodies.<sup>45, 110</sup> Aptamers are single stranded nucleic acid chains that can be designed with high affinity for a target through systematic evolution of ligands by exponential enrichment (SELEX).<sup>45, 110</sup> As with antibody recognition elements, label-free aptamer

sensors are desirable to reduce time and complexity. Label-free aptamer detection has often relied on coating screen-printed electrode surfaces with nanocomposites containing redox indicators for voltammetric detection and nanomaterials for probe immobilization and enhancement of electrode kinetics.<sup>45, 110</sup> An aptamer-based ePAD was developed for simultaneous detection of CEA and neuron-specific enolase (NSE) cancer biomarkers. An amino functional graphene-Thionin (THI)-Au nanoparticle nanocomposite electrode was used for CEA detection and a Prussian blue (PB)-poly(3,4-ethylenedioxythiophene) (PEDOT)-Au nanoparticle composite electrode was used for NSE detection. The modifications improved electron transfer kinetics and allowed for NSE and CEA aptamer immobilization through thiol-Au attachment. THI and PB indicators were detected with DPV and decreased current intensity occurred when the analytes bound to the aptamers.<sup>45</sup> PNA are uncharged synthetic mimics to natural nucleic acid chains.<sup>25, 117</sup> Their neutral charge backbone gives them an advantage over natural nucleic acid probes by eliminating electrostatic repulsion which lowers the background signal for hybridization-induced EIS detection.<sup>117</sup> PNA probe hybridization has been utilized to detect a 15-base oligonucleotide of *Mycobacterium tuberculosis* (MTB) with  $[\text{Fe}(\text{CN})_6]^{3-/4-}$  mediator and EIS. For this ePAD, the PNA probe was immobilized on partially oxidized cellulose folded over the electrode instead of the electrode itself allowing regeneration by PAD replacement.<sup>25</sup> For binding DNA targets without the need for prior generation of single strands, triplex forming oligonucleotides (TFO) have been used on ePADs for methylene blue-labeled detection.<sup>116</sup> A recent report by Kokkinos et al. has also utilized ASV for determination of target DNA with nucleic acid probes.<sup>118</sup> Capture DNA were immobilized onto a Sn-sputtered working electrode, hybridized with biotinylated target DNA, which were then labeled with streptavidin-conjugated CdSe/ZnS quantum dots. HCl was added to oxidize the quantum dots and release Cd(II) which was detected with ASV to quantify the target DNA.<sup>118</sup>

Other less established electrochemical affinity assay recognition elements used in the ePAD literature include molecularly imprinted polymers (MIPs)<sup>40, 119, 120</sup> and cell-based biosensors.<sup>121</sup> MIPs mimic natural biorecognition elements and can have antibody-like binding affinities toward analytes of interest but are cheaper and more robust.<sup>48</sup><sup>119</sup> MIPs are typically made by polymerizing monomers in the presence of a target molecule then extracting the targets leaving microcavities for rebinding targets.<sup>122</sup> The ePAD electrode can be used as a platform to synthesize MIPs through dropcasting reactants onto electrodes to form a MIP film<sup>48</sup> or through electropolymerization of MIPs

on the working electrode surface.<sup>120</sup> A report by Chi et al. used chitosan-modified electrodes to adsorb CEA and dopamine was electropolymerized around the CEA target to molecularly imprint the electrode for label-free DPV detection of CEA (Fig. 6).<sup>120</sup> A recent paper by Sun et al. combined MIPs into an ePAD to detect glycoprotein ovalbumin (OVA) in a sandwich assay format for sub pg/ml detection limits.<sup>48</sup> MIPs have also been incorporated into ePADs through the addition of MIP nanobeads. MIP nanobeads have been used in paper-based platforms for simple potentiometric sensing of bisphenol A, an antagonist for estrogen receptors prevalently found in the environment.<sup>119</sup> The first cell-based ePAD biosensor was developed for the detection of casein, an allergen in milk. Basophilic leukemia (RBL-2H3) mast cells were immobilized on a paper-based electrode surface for their ability to recognize and have proinflammatory responses to food allergens. The mast cell responses to casein were monitored with DPV.<sup>121</sup>

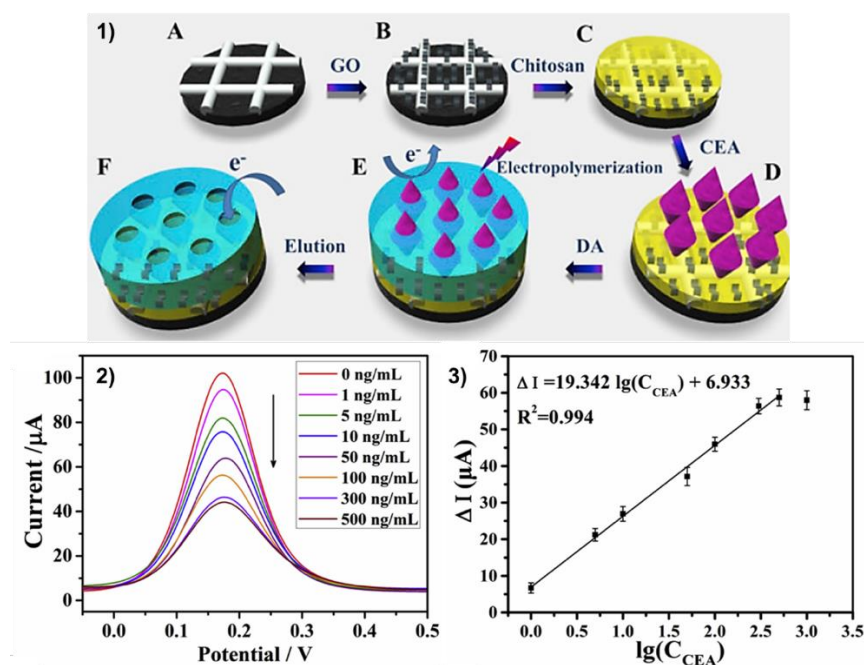


**Fig. 6** MIP ePAD for label-free detection of CEA. 1) Electrode modification: carbon ink electrode is modified with graphene oxide (A-B), chitosan is dropcasted (C) CEA is adsorbed to chitosan (D) dopamine is electropolymerized around the CEA (E) CEA is removed leaving a MIP-modified ePAD (F). 2-3) DPV of 5 mM  $[\text{Fe}(\text{CN})_6]^{3-/4-}$  on ePADs modified with 0-500 ng/mL CEA and CEA calibration curve. Reprinted with permission from ref<sup>120</sup>: J. Qi, B. Li, N. Zhou, X. Wang, D. Deng, L. Luo, L. Chen, *Biosens. Bioelectron.*, 2019, **142**, 111533 (Copyright 2019 Elsevier)

#### 4.5. Electrochemiluminescent detection

In electrochemiluminescence (ECL), light emission is produced by species that are promoted to excited states due to a preceding electrochemical reaction. As opposed to previously described electrochemical detection where current is measured after potential is applied on the electrode, intensity of light emission is measured in ECL. For low-cost applications, a phone camera or custom-built photomultiplier tube (PMT) detector can be used for signal readout.<sup>123, 124</sup> ECL can be generated in two ways: 1) via annihilation, where the electron transfer reaction occurs between an oxidized and a reduced species, both produced at the electrode by pulsing the electrode potential between appropriate states and 2) via bimolecular electrochemical reactions between the luminophore (i.e. species that can undergo light emission) and a co-reactant.<sup>125</sup> Similar to photoluminescence (PL) technique, ECL provides a temporal and spatial control of light emission. However, the absence of excitation light in ECL provides superior signal-to-noise level compared to PL.

ECL was first demonstrated in paper-based format by Delaney and coworkers using screen-printed electrodes and tris(2,2'-bipyridyl)ruthenium(II) ( $\text{Ru}(\text{bpy})_3^{2+}$ ) as a luminophore to detect 2-(dibutylamino)-ethanol (DBAE) and nicotinamide adenine dinucleotide (NADH).<sup>124</sup> Both DBAE and NADH can separately act as co-reactants for  $\text{Ru}(\text{bpy})_3^{2+}$  and thus are able to provide a dose-response signal via ECL. Although  $\text{Ru}(\text{bpy})_3^{2+}$  has been widely used for commercial application of ECL, the broad emission bands of the luminophore may restrict application of this ECL label for simultaneous multianalyte determination on paper-based devices.<sup>126</sup> In addition, it is often difficult to directly label antibodies using  $\text{Ru}(\text{bpy})_3^{2+}$  for immunoassay application due to the absence of functional groups on the inorganic molecule. Synthesis of  $\text{Ru}(\text{bpy})_3$ -NHS ester have been reported for conjugation of this ECL luminophore to protein.<sup>127</sup> However, the synthesis and purification of reaction product from the remaining reactants can take a significant amount of time. Fortunately, nanoparticles provide more opportunities to widen the applications of ECL by serving as: 1) a carrier platform for inorganic ECL labels,<sup>128, 129</sup> 2) luminophores,<sup>129, 130</sup> 3) energy acceptors to quench ECL reaction,<sup>131, 132</sup> and 4) electrocatalysts for ECL reactions.<sup>133, 134</sup> Many nanoparticles-based ECL labels have been reportedly used in paper devices to date including semiconductor nanocrystal/quantum dots (QDs) (e.g. CdTe QDs, CdSe QDs), metal nanoparticles (NPs) (e.g. Pt-AuNPs, Pd@AuNPs), carbon dots, graphene QDs and carbon-nanocrystals (CNCs).<sup>135</sup>

Sandwich immunoassays are commonly coupled with paper-based ECL for biomarkers detection, where the primary antibody is immobilized on the surface of screen-printed carbon electrodes.<sup>136, 137</sup> This strategy is often preferred for fabricating disposable paper devices due to the ease and low cost of electrode manufacturing. Ru(bpy)<sub>3</sub><sup>2+</sup>-labeled secondary antibody is then added sequentially after the analyte is captured by the primary antibody. To enhance conductivity and increase surface area for primary antibody immobilization, Gao et al. grew AgNPs on the surface of paper substrate to create a paper working electrode (PWE).<sup>138</sup> They also employed Au nanocages to adsorb Ru(bpy)<sub>3</sub><sup>2+</sup> and conjugate the secondary antibody. Using this Ru(bpy)<sub>3</sub><sup>2+</sup>-labeled Au nanocages, a sub-pg/mL detection limit was achieved for CEA. PWE was also implemented by Yan and coworkers using AuNPs for aptamer immobilization on their paper-based ECL device.<sup>139</sup>

To create a simple, yet sensitive paper-based ECL, bipolar electrodes (BPEs) can be implemented.<sup>52, 140, 141</sup> BPEs are electronic conductors that are in an ionic phase between anode and cathode without physical contact to an external power supply. When a sufficiently high electric field is applied across this ionic phase, faradaic processes occur at the ends of the BPE and ECL can be used as an indirect reporter of this faradaic process. The ability of BPE to modulate the local electric field within microfluidic channel also allows for enrichment of charged analytes at the poles of BPE for sensitive detection.<sup>142, 143</sup> Screen-printed carbon (SPC) electrodes are commonly used to construct BPEs and a few groups reported on modifying the SPC-BPE with AuPd NPs and multi-walled carbon nanotubes to enhance ECL responses.<sup>52, 140</sup> Ge and coworkers used AuPd NPs-modified BPE to serve as a carrier for capture aptamers and catalyst for ECL reaction between luminol and H<sub>2</sub>O<sub>2</sub> for detection of tumor cells.<sup>52</sup> Once the tumor cells were captured by the aptamer, a secondary aptamer and two hairpin structure DNA labeled-luminol/AuNPs were added to initiate in-situ hybridization chain reaction (Fig. 7). This chain reaction allowed for accumulation of luminol on the electrode to react with H<sub>2</sub>O<sub>2</sub> released by the cells. A detection limit of 40 cells/mL was reported using this assay scheme. Similar BPEs-based aptasensor targeting CEA was reported by Zhang et al. by incorporating patchy Au-coated Fe<sub>3</sub>O<sub>4</sub> nanospheres to enhance the catalytic activity of the electrodes.<sup>144</sup>

Three-dimensional (3D) devices may provide suitable platforms for multiplexing and control in multistep assays to be performed in paper-based ECL. For example, Sun et al. performed a multistep ECL-immunoassay on a rotational paper-based device for simultaneous detection of CEA and prostate specific antigen (PSA).<sup>137</sup> The

device consists of multiple paper discs that can be rotated to obtain device configurations allowing for addition of reagents and washing buffers. Similar multistep control was reported by Yang et al. using sudoku-like folding paper devices to enhance ECL signal from graphene QDs using semicarbazide and AgNPs.<sup>145</sup> Fluidic control via 3D paper device was also utilized by Huang and coworkers to perform auto-cleaning on their working electrodes.<sup>47</sup>

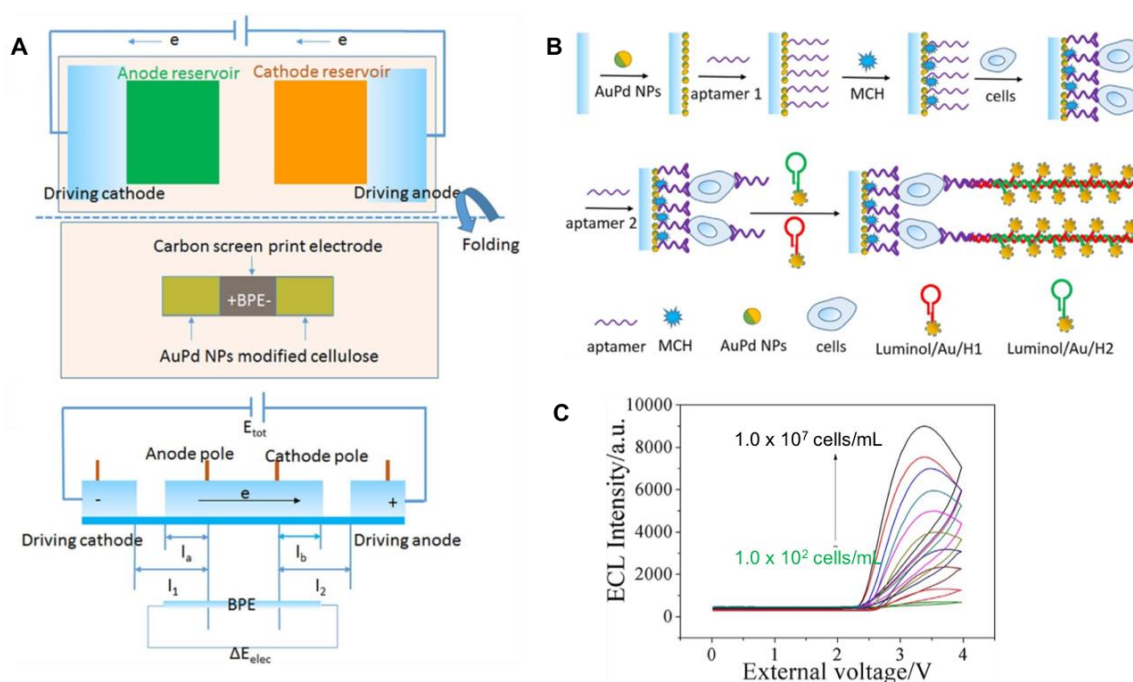


**Fig. 7** Paper-based BPE for ECL detection of tumor biomarkers: (A) Schematic illustration of paper-based BPE and potential difference across the BPE, (B) Assembly process of the cytosensor and (C) ECL intensities of the sensors at different concentrations of MCF-7 cells. Adapted with permission from ref<sup>52</sup>: S. G. Ge, J. G. Zhao, S. P. Wang, F. F. Lan, M. Yan and J. H. Yu, *Biosens. Bioelectron.*, 2018, **102**, 411-417 (Copyright 2018 Elsevier).

Multiplexing was reported by Wu et al. and Ge et al. for detection of cancer cells and tumor biomarkers, respectively, by stacking or folding multiple layers of paper.<sup>134, 136</sup> In both cases, multiplexing was achieved by spatially resolving the detection at different test zones that are connected to a single inlet for sample addition. While this strategy is frequently implemented, dividing the sample into multiple detection zones can compromise assay sensitivity depending on the ratio of analyte present at the detection zone to the total analyte present in the sample. Sample loss to the paper<sup>146</sup> should also be considered when designing such multiplexing devices. Zhang and coworkers implemented a potential-control technique for simultaneously detecting Pb<sup>2+</sup> and Hg<sup>2+</sup> on a single working electrode using two ECL labels (Ru(bpy)<sub>3</sub><sup>2+</sup> at AuNPs and CNCs-coated SiNPs) which operate at different

applied potentials.<sup>147</sup> A similar strategy was also reported using  $\text{Ru}(\text{bpy})_3^{2+}$  and carbon nanodots as ECL labels to detect tumor markers.<sup>148</sup>

## 5. Applications

The primary goal in developing the microfluidic paper-based analytical devices is making a sensor that can rapidly and accurately quantify analytes in the field at a low cost. Since electrochemical methods were first applied to paper-based devices for the detection of glucose, lactate, and uric acid,<sup>8</sup> various analytes have been targeted with ePADs. Table 1 summarizes the recent ePADs applications including target analytes, sample matrices, the applied electrochemical methods, and associated limits of detection. ePADs were used for clinical diagnosis, environmental testing, food analysis, and drug analysis. Recent ePADs applications not only show the applicability to detect various analytes but also demonstrate the possibility of multiplexing through origami and channel geometry design. Multiplexed devices can increase the efficiency and precision of the analysis. For example, several analytical methods can be integrated into a single device and sequentially applied by using the origami method.<sup>53, 54</sup> In these devices, colorimetric, electrochemical, and electrochemiluminescent detection can be performed on separate paper layers. Each detection method was used to target a single analyte. Other ePADs transport the sample to detection regions that have independent electrodes through the flow channel (Fig. 8A-B).<sup>17, 35, 36, 39</sup> This method allows for detection of different analytes simultaneously from a single sample addition. de Oliveira et al. implemented simultaneous multi-analyte detection by separating a sample loading zone without using a flow channel (Fig. 8C).<sup>29</sup> Finally, independent ePADs were connected to a multiplexed electrochemical platform to analyze various samples simultaneously (Fig. 8D).<sup>16</sup>

**Table 1.** Recent ePAD applications for clinical diagnosis, environmental testing, and analyses of food, drug and chemical warfare agent

Analyte	Sample type	Electrochemical technique	Detection limit	Ref
<b>Clinical Diagnosis</b>				
Glucose	Human serum	Chronoamperometry	0.67 $\mu$ M	19
	Sweat	Amperometry	5 $\mu$ M	46
	Urine	Chronoamperometry	0.3 $\mu$ M	35
C-reactive protein	Human plasma	Electrochemical impedance spectroscopy	0.001mg/L	50
	Human serum	Electrochemical impedance spectroscopy	15 ng/mL	49
Milk allergen casein	Rat basophilic leukemia mast cells	Differential pulse voltammetry	0.032 $\mu$ g/mL	121
microRNA	Human serum	Differential pulse voltammetry	0.35 fM	149
	Human serum	Differential pulse voltammetry	0.43 fM	40
M. tuberculosis genomic DNA	Human whole blood/serum	Square wave voltammetry	0.04 ng/ $\mu$ L	27
17 $\beta$ -estradiol	Human serum	Differential pulse voltammetry	10 pg/mL	39
Carcinoembryonic antigen (CEA) Prostate specific antigen (PSA)	Human serum	Electrochemiluminescence	0.07 ng/mL (CEA) 0.03 ng/mL (PSA)	137
DNA	Standard solutions	Anodic stripping voltammetry	0.11 pM	118
Single-stranded and double-stranded DNA	Human serum	Square wave voltammetry	3 nM (single) 7 nM (double)	116
Glycoprotein ovalbumin	Egg white	Differential pulse voltammetry	1 pg/mL	48
Adenosine triphosphate (ATP)	Human serum	Differential pulse voltammetry	0.08 $\mu$ M	150
Butyrylcholinesterase	Human serum	Chronoamperometry	0.5 IU/mL	24
Human interferon-gamma (IFN- $\gamma$ )	Human serum	Electrochemical impedance spectroscopy	3.4 pg/mL	74
Norepinephrine (NE) Serotonin (5-HT) p-aminophenol(pAP)	Standard solutions	Differential pulse voltammetry	1.2 $\mu$ M (NE) 0.38 $\mu$ M (5-HT)	17
PSA	Human serum	Differential pulse voltammetry	10 pg/mL	110
Cl <sup>-</sup>	Human serum and sweat	Cyclic voltammetry	1 mM	20
Serotonin	Urine	Linear sweep voltammetry	2 nM	32
Uric acid and creatinine	Urine	Square wave voltammetry	8.4 nM (uric acid), 3.7 nM (creatinine)	36
West Nile Virus	Kidney cells	Electrochemical impedance spectroscopy	10 virus particles/50 $\mu$ L media	66
MCF-7 cancer cell	Human serum	Differential pulse voltammetry	20 cells/mL	54
<b>Environmental Testing</b>				
Pesticides	River water	Chronoamperometry	50 ppb	55
Ethinylestradiol	River and tap water	Square wave voltammetry	0.1 ng/L	114
Cd(II), Zn(II)	Standard solutions	Anodic stripping voltammetry	1 $\mu$ g/L	28
Cd(II)	Standard solutions	Square wave anodic stripping voltammetry	not specified	42

Analyte	Sample type	Electrochemical technique	Detection limit	Ref
Pb(II)	Tap and river water	Electrochemiluminescence	0.14 nM	53
Formaldehyde	Artificial wastewater	Chronoamperometry	not specified	151
Hg(II)	River water	Linear sweep voltammetry	30 nM	18
<b>Food Analysis</b>				
Ascorbic acid	Commercial tablets	Square wave voltammetry	70 $\mu$ M	69
	Dietary supplements	Cyclic voltammetry	0.15 mM	60
Glucose	Soft drinks	Coulometry	0.33 mM	152
	Soft drinks	Linear sweep voltammetry	6 $\mu$ M	72
	Fruits and beverages	Chronoamperometry	0.4mM	16
Tertiary butylhydroquinone	Edible oils	Differential pulse voltammetry	12 nM	153
<b>Drug Analysis</b>				
Ascorbic (AA), paracetamol (PAR), and caffeine (CAF)	Commercial tablets	Square wave voltammetry	0.40 mM (AA), 0.04 mM (PAR), 0.22 mM (CAF)	29
Prednisolone (PRED), dexamethasone (DEX)	Herbal medicines	Differential pulse voltammetry	12 $\mu$ g/mL (PRED), 3.6 $\mu$ g/mL (DEX)	37
<b>Chemical Warfare Safety</b>				
Sulfur mustard	Standard solutions and aerosol	Amperometry	1 mM (liquid), 0.019 g·min/m <sup>3</sup> (aerosol)	51

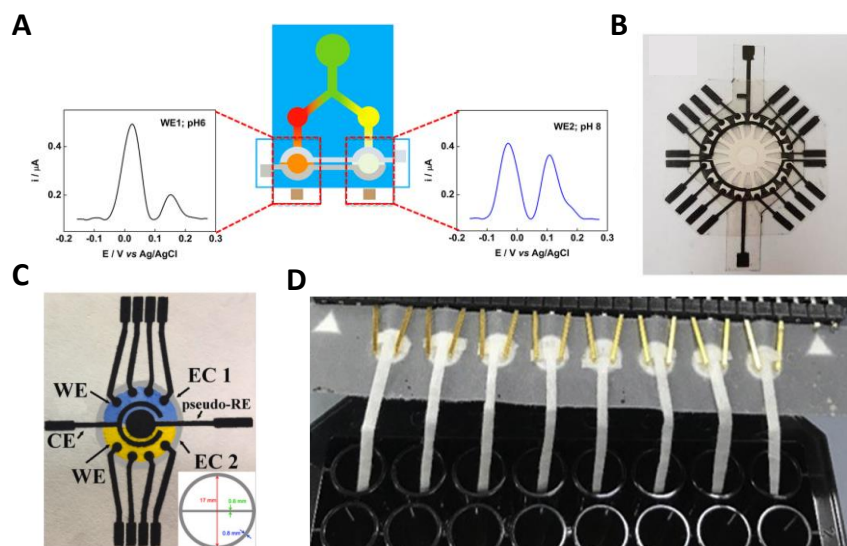


**Fig. 8** Multi-multiplexed ePADs: Independent detection region through (A) 2 and (B) 16 flow channels. Reprinted with permission from ref<sup>7</sup>: S. Nantaphol, A. A. Kava, R. B. Channon, T. Kondo, W. Siangproh, O. Chailapakul and C. S. Henry, *Anal. Chim. Acta*, 2019, **1056**, 88-95 (Copyright 2019 Elsevier) and ref<sup>35</sup>: E. L. Fava, T. A. Silva, T. M. do Prado, F. C. de Moraes, R. C. Faria and O. Fatibello-Filho, *Talanta*, 2019, **203**, 280-286 (Copyright 2019 Elsevier). (C) Separate electrochemical cells containing 4-working electrodes each. Reprinted with permission from ref<sup>29</sup>: T. R. de Oliveira, W. T. Fonseca, G. D. Setti and R. C. Faria, *Talanta*, 2019, **195**, 480-489 (Copyright 2019 Elsevier). (D) Simultaneous measurement of 8 samples. Reprinted with permission from ref<sup>16</sup>: O. Amor-Gutierrez, E. Costa-Rama and M. T. Fernandez-Abedul, *Biosens. Bioelectron.*, 2019, **135**, 64-70 (Copyright 2019 Elsevier).

## 6. Progress toward practical applications

The global market size for paper diagnostic was estimated at USD 5.69 billion in 2017 and projected to reach over USD 9 billion in 2025.<sup>154</sup> The majority of these paper diagnostics are in lateral flow and dipstick formats whose technologies had been established much earlier than paper-based microfluidics.<sup>3, 155</sup> Many applications including blood typing, urinalysis and disease diagnostics have been targeted by commercial and prototyped paper sensors made by ARKRAY, Inc.; Acon Laboratories, Inc.; Abbott; Bio-Rad Laboratories; Siemens Healthcare GmbH; Haemokinesis; INSiGHT; and Diagnostics for All.<sup>6, 154</sup> Although the glucose meter has been around for decades as a successful prototype of point-of-care electrochemical sensors,<sup>156</sup> there has not been any commercialized ePAD reported to date. There could be a number of factors contributing to the absence of commercial ePAD such as difficulty in meeting all ASSURED criteria set by WHO,<sup>157</sup> limitations in mass-producing the devices, and the lack of funding and industrial partners bridging the gap between assay development and commercialization. With the growing market of medical diagnostics in general, more opportunities are expected to open for funding and collaboration between academic researchers and industrial counterparts to bring paper-based point-of-care testing (POCT) including ePADs to customers. Thus, it is critical to address the analytical and practical specifications required for POCT before delivering these devices for any intended applications. The following sections highlight major milestones achieved within ePAD field in meeting those required specifications and our critical outlook on the current technologies and what is necessary for moving forward.

### 6.1. Analytical figures of merit

Affordability is undeniably one major selling point for paper-based POCT. However, analytical performance is often not something that can be compromised to achieve the low-cost goals. Depending on the application, whether the assay is intended to be semi-quantitative or quantitative, if the target is a specific analyte or a group of analytes, and the nature of the sample and target analytes, the required figures of merit can vary significantly. We examined how these important analytical figures of merit (such as limit of detection, sensitivity, selectivity, precision, and accuracy) have been addressed in ePADs.

### **Limit of detection (LOD) and sensitivity**

Since the first published work on ePADs,<sup>8</sup> many efforts have been dedicated to improving detection limits and sensitivity of the electrochemical sensors to make them suitable for POCT applications. Strategies include selection and modification of electrode material,<sup>54, 158</sup> optimization of electrochemical methods used for measurements,<sup>40, 66, 118</sup> innovation in device configuration,<sup>42, 159, 160</sup> and utilization of enzyme-substrate pairs and nanoparticles for signal amplification.<sup>54, 118, 160</sup> It is often difficult to understand what aspect of an assay contributes the most in improving sensitivity, especially in a hybrid device that utilizes a novel electrode material, device configuration and detection approach at the same time. This type of investigation may sometimes be overlooked as the focus of ePAD research is directed towards the analytical specifications being achieved. However, recognizing major factors that dictate performance of ePADs could provide a better insight into how to create more efficient, yet powerful analytical devices. One- to two-orders of magnitude improvements in sensitivity have been achieved by switching from single-layer to multilayer paper devices<sup>42</sup> and electrode modification with nanocomposites.<sup>39, 74, 161</sup> The use of pulse and stripping voltammetry to achieve lower LODs has also been well documented.<sup>28, 54, 114, 149</sup> While there are multiple ways of improving the sensitivity of ePADs, choosing the simplest approach whenever applicable could save some time and resources, reduce assay complexity, and improve reproducibility.

Sub-nanomolar detection limits of disease biomarkers in ePADs have been reported,<sup>40, 74, 110</sup> showing comparable performance of state-of-art ePADs to conventional bench-top instrumental methods used in clinical settings. Promising ppb LODs have also been reported by ePADs targeting metal and organic contaminants in food and environmental samples.<sup>55, 118, 162</sup> One of challenging tasks in POCT application is creating a tool for rapid pathogen (bacteria and viruses) detection that also meets the very strict LOD requirements set up by regulatory agencies. For example, the Environmental Protection Agency (EPA) sets a maximum contaminant level goal (MCLG) for microbial contaminants that possess threat to public health at zero per 1 L of drinking water.<sup>163</sup> This means that the applicable method has to be able to detect single pathogen. Very low detection limits (1-15 cfu/mL) have been achieved by several electrochemical immunosensors reported in the past decade.<sup>164, 165</sup> Adapting these technologies and combining them with some advantages of paper microfluidics to perform sequential reagent

delivery for multiple steps assays<sup>166-168</sup> and/or samples preconcentration<sup>169-171</sup> could be a potential way to design an ePAD for such applications.

### Selectivity

To achieve the highest degree of selectivity in ePADs, utilization of protein and nucleic acid-based recognition elements is common.<sup>49, 110, 114, 137, 172</sup> Antibody-based immunosensors have been widely used in laboratory and POC testing. Aptamers, as an emerging alternative, have also gathered interest and potential applications in the field, especially for targeting small molecules. Molecularly imprinted polymers (MIPs), although they have not been widely used for ePAD, could also be an attractive material for achieving selectivity.<sup>32, 48, 173, 174</sup> In addition to the ease of mass preparation, MIPs also have better physical and chemical stability over antibodies. Other reported approaches to obtain selectivity on ePAD include electrode modification with ion selective membranes and selective catalyst, performing online separation on paper, and optimization of applied waveforms.<sup>8, 55, 70, 175</sup> While these approaches are often simpler and/or less expensive to execute, the applications could be limited by complexity of sample matrices as interferents with similar properties to the target analyte could exist. The use of specific recognition elements is still preferable to achieve selectivity in complex biological matrix, whereas the later mentioned approaches are great alternatives for testing environmental and other sample types where the effect of interferents to analyte detection is not severe.

Assay selectivity on ePADs can be showcased by performing an interference study.<sup>20, 32, 53, 175</sup> In this study, multiple possible interferents are tested separately, in the presence of analyte, to assess how detector response changes as a function of interferent quantity and the tolerance ratio. Tolerance ratio is a ratio of interferent to analyte that causes  $\pm 5\%$  alteration to the original signal in absence of interferent.<sup>175</sup> Interference studies are particularly useful for identifying substances that could be detrimental to analyte detection and perform corrective action to remove the interferents.<sup>175</sup> Interference studies are often not demonstrated in electrochemical paper sensors that employ specific recognition elements such as antibodies and aptamers. However, negative control experiments with nonspecific analytes of the same type (i.e. other small molecules, macromolecules, or cells, etc.) are still necessary to validate assay specificity.<sup>40, 66, 118</sup> Although it is not a common practice, performing interference studies in

immunosensors would provide an additional information on how analyte detection is affected by other non-target substances.<sup>39, 110</sup>

### **Precision**

Repeatability and reproducibility are often used as indicators of method precision. Repeatability measures variation from performing the assay under the same conditions (same operator, testing location, measurement procedure, and instrument) and repetition is typically over a short period of time. Reproducibility, on the other hand, refers to the agreement between experimental results conducted by different individuals, at different locations or with different instruments. Thus, reproducibility is a stronger indicator on how the proposed ePAD would perform for POCT. Since many of the reported ePADs are still in the development stage, it is understandable that there is often not much information provided on the reproducibility of the assays. However, this is something that should be assessed prior to bringing the technology out of the laboratory. Less than 5% relative standard deviations (RSDs) have been reported in repeatability studies in recently developed ePADs.<sup>48-50, 55, 121</sup> Sources of variability within different devices measurements can include (but are not limited to) imprecision in device geometry, electrode size, amount of deposited reagents, and volume of sample added to the devices. More controlled and preferably automated ePAD fabrication would potentially reduce this variability. Random error is expected to increase as the assay is employed in the field and at POC due to variation in assay conditions. Thus, it is very important to create a validated protocol for the assay, determine the range of working conditions at which the assay will perform as previously tested and validated in the lab, and establish necessary correction factor to account for variability in testing conditions.

### **Accuracy**

The level of accuracy required for analytical methods depends on the analyte levels and the application. One way to express the accuracy of a proposed analytical method is by establishing a correlation between results of the proposed and the reference methods. When the results are not statistically different at a given level of significance, linear regression comparing both methods should yield a straight line of approximately unity slope and zero intercept.<sup>176</sup> Another way to express method accuracy, especially when dealing with complex sample matrices, is by performing a recovery study. Acceptable recovery percentages for a laboratory method vary from 98-102% at

analyte level of 100% to 40-120% for 1 ppb level of analyte.<sup>177</sup> This metric gets complicated when comparing a small molecule or even an elemental target analyte to a macromolecule such as protein or genomic DNA as the molecular weights differ greatly. Some recovery values reported from ePADs targeting clinical diagnostic applications are summarized in Table 2. Recovery values ranging from 80% to 103% were also reported for trace analysis of metals and pesticides at ppb and sub-ppb levels in environmental samples.<sup>53, 55, 178</sup> These results are encouraging and demonstrate that the current ePAD technology strives to meet the necessary analytical requirements. The accuracy requirement is also typically less demanding for a field or POC testing that is intended for screening or quick monitoring purposes. For example, the current guidance for blood glucose meter by US Food and Drug Administration is 95% of all measured values must be within 15% of the true value (i.e. value from a lab measurement) and 99% of meter values must be within 20% of the true value.<sup>179</sup>

Variability in sample matrices is a factor to consider when translating ePAD technology for real world applications. For example, pH, protein level, and viscosity can vary in urine, serum, saliva samples from different patients. All these variables could impact analyte diffusion to the electrode, binding to receptor and the rate of redox reaction which affects the measured electrochemical signal. Ensuring the proposed assay is robust and relatively unaffected by these matrix-related properties would provide more assurance on the accuracy of the test.

**Table 2.** Recovery percentages of ePAD detection on several diagnostic markers

Analyte	Sample matrix	Recovery (%)	Concentration tested	Ref
C-reactive protein	serum	98-104	5.0-40.0 $\mu\text{g/mL}$	60
Serotonin	urine	100-111	0.1-0.5 $\mu\text{M}$	32
PSA	serum	92-109	1.1-78.7 $\text{ng/mL}$	110
ATP	serum	96-104	1.0-5.0 $\mu\text{M}$	150
CEA	serum	92-108	2.5-14.9 $\text{ng/mL}$	137
17 $\beta$ -estradiol	serum	92-115	0.025-1.7 $\text{ng/mL}$	39
miRNA-21	serum	99-101	1.0 fM-1.0 pM	40
miRNA-155	serum	94-100	1.0 fM-1.0 nM	149
IFN- $\gamma$	serum	101-104	50-500 $\text{pg/mL}$	74

## 6.2. Mass production feasibility

When considering scalability of ePAD fabrication for mass production, there are at least three fabrication aspects that need to be considered: 1) patterning microfluidic channels, 2) deposition of assay components including electrodes, and 3) construction of multilayered geometry (if applicable). Each step will also dictate cost of the final device.

A vast selection of techniques for patterning microfluidic channels on paper substrate have been described in review articles.<sup>5, 180</sup> Printing-based techniques are popular due to their simplicity, easily automated process and compatibility with paper substrates. Traditional methods such as screen-, flexographic- and gravure-printing are superior for large-scale production of paper microfluidics. However, these methods often require costly infrastructure and are not readily adaptable for new device designs. Patterning paper using a wax printer is plausibly the most common in ePAD fabrication. In addition to being low-cost (i.e. less than \$1000 for the printer and costs ~\$0.001/cm<sup>2</sup> printing on Whatman chromatography paper)<sup>15</sup> and suitable for prototyping, mass production is possible with this technique. The major downside of using wax for printing, however, is its incompatibility with liquids or solutions with low surface tension such as organic solvents and surfactants. Inkjet printing using ink materials that can resist these types of liquid/solution is an alternative to mass produce paper devices for such applications at low cost. The use of silicon resin and hydrophobic sol-gel derived methylsilsesquioxane as inks has been reported.<sup>181, 182</sup>

Similarly, there are multiple techniques reported for electrode fabrication on paper substrates. Screen- and stencil-printing are among the common methods to mass produce electrodes. Using a carbon-based ink, electrodes can be patterned as low as ~0.01 USD. Other types of conductive inks including Ag and Au inks have been used for screen-printing.<sup>183-185</sup> Inkjet printing, despite not being as popular as screen-printing, is a great alternative for producing electrodes with higher resolution at large scales. In addition, inkjet printing can also be employed to fabricate the whole ePAD components including hydrophobic barrier, electrodes and reagents necessary to complete the assay on paper substrate. Such application has been demonstrated by Citterio group.<sup>62</sup> The group also published excellent reviews on inkjet printing technology for paper-devices.<sup>186, 187</sup>

Multilayered geometry within ePAD allows for additional functionality including control for multiple assay steps, tuning flow rates and flow direction, and multiplexing.<sup>42, 137, 160</sup> However, fabricating such device in large scales may pose significant hurdle and introduce imprecision. Adhesive tape-based 3D devices are often difficult to manufacture due to the necessity to precut and sometimes manually align components of the device. Folding/origami devices are more adaptable to mass production as the entire device can be fabricated on a single sheet of paper.<sup>188</sup> Combining this folding strategy with lamination also eliminates the need of tape to hold the multiple layers of paper together.<sup>189</sup>

### **6.3. Viability for field and POC testing**

#### **Portability**

One important aspect that dictates whether a testing tool is suitable for field or POC applications is portability. While the proposed paper devices are generally small, most of the electrochemical measurements were done using a benchtop potentiostat that is not ideal for POCT. A year after the first published ePAD, the Whitesides group reported an ePAD design that used a commercial glucometer as an electrochemical reader.<sup>190</sup> Not only does the paper strip give comparable performance to the commercial test strip for glucose measurement, it also costs 30 times less which demonstrates how promising paper-based sensors are for POCT. A 3D pop-up paper device that works with the similar commercial meter was also reported by the group for measuring beta-hydroxybutyrate (a biomarker for diabetic ketoacidosis).<sup>191</sup>

Although the glucometers are inexpensive, they are limited to amperometry measurement. Some companies including Palmsens, Metrohm and DropSens sell portable potentiostats that are either battery-powered or powered via USB, and can perform several electrochemical techniques.<sup>192</sup> However, these potentiostats typically cost thousands of dollars, which is expensive especially for the use in resource-limited setting. To overcome the issue, the Plaxco group introduced an open-source, do-it-yourself (DIY) potentiostat in 2011.<sup>193</sup> This handheld potentiostat costs less than \$80 to build and supports a number of waveforms for performing several voltammetry techniques. The technology has since been further developed by researchers in the field to allow for more functions including wireless communication to smartphone or tablet, chemometric data processing, multiplexed readout etc.<sup>87, 194, 195</sup> Table 3 summarizes some of these reported custom-built potentiostats and their key features. Pal and coworker

also reported a self-powered ePAD where they integrated a hydrophobic paper-based triboelectric generator that can recharge their battery-powered potentiostat via pressure applied to the device by the user.<sup>196</sup> With this emerging technology, cost for performing ePAD-based measurements in the field or at POC is not a huge barrier anymore.

**Table 3.** Portable custom-built potentiostats and their key features

Potentiostat	Cost (\$)	Features	Ref
CheapStat	<80	Open source (software and hardware); computer-device interface via USB; supports cyclic, square wave, linear sweep and anodic stripping voltammetry	193
Multichannel potentiostat (1) (Fig. 9A)	~90	Computer-device interface and powered via USB; simultaneous measurement at up to 8 electrodes, support amperometry and voltammetry (cyclic)	87
Multichannel potentiostat (2)	Not reported	Real-time measurement of amperometric signals from up to 48 electrodes	197
uMED	~25	Compatible with low-end and smartphones (audio cable connection); compatible with several commercially available and paper-based electrodes; supports amperometry, coulometry, voltammetry, potentiometry; supports on-board sample mixing	198
DStat	~120	Open source; pA current measurement capabilities; computer-device interface via USB; supports potentiometry, amperometry, voltammetry (cyclic, differential pulse, square wave)	199
Potentiostat + smartphone-based multivariate analysis	Not reported	Battery-powered; wired and wireless connection to smartphone; supports on-site data processing using principle component analysis; data sharing via cloud; supports cyclic voltammetry	195
USB-controlled potentiostat/galvanostat	~95	Open source; computer-device interface via USB; wide potential range ( $\pm 8V$ ); suitable for battery characterization	200
PSoC-Stat	~10	Open source; uses a single commercially available integrated circuit (easier to build by untrained user); computer-device interface via USB; supports amperometry, cyclic and anodic stripping voltammetry	201
UWED (Fig. 9B)	~60	Open source; wireless connection to smartphone/tablet via Bluetooth; uses phone for both user interface and data storage via cloud; powered by rechargeable battery; supports potentiometry, chronoamperometry, cyclic and square wave voltammetry	194

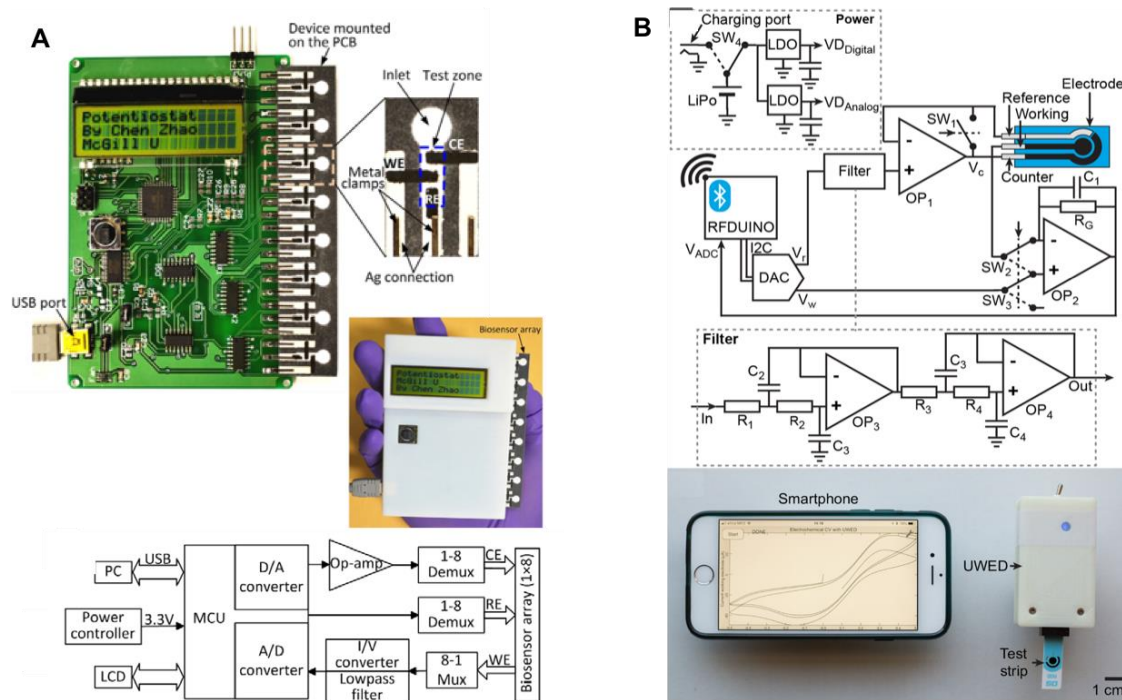


**Fig. 9** Portable potentiostats: (A) Multichannel potentiostat- (top) device architecture and image with 8 measurement channels for ePADs, (bottom) circuit diagram of the device. Adapted from ref<sup>87</sup>: C. Zhao, M. M. Thuo and X. Liu, *Sci. Technol. Adv. Mater.*, 2013, **14**, 54402-54402 (B) Universal wireless electrochemical detector (UWED)- (top) circuit diagram and main components of the device, (bottom) image of UWED paired with smartphone application to perform measurement on a test strip. Adapted with permission from ref<sup>194</sup>: A. Ainla, M. P. Mousavi, M. N. Tsaloglou, J. Redston, J. G. Bell, M. T. Fernández-Abedul and G. M. Whitesides, *Anal. Chem.*, 2018, **90**, 6240-6246 (<https://pubs.acs.org/doi/abs/10.1021/acs.analchem.8b00850>). Further permissions related to the material excerpted should be directed to the American Chemical Society.

## Stability

Making sure that ePADs are stable for a reasonable storage period is one critical step that has to be addressed before deploying these sensors for POCT. These devices are typically developed in laboratories with controlled temperature and humidity whereas these two parameters are hard to control in the field or at POC. Thus, performing stability studies under different storage conditions including elevated temperature and high humidity should be performed. Commercial products such as glucose strips and urine dipsticks typically have shelf-life around 18-24 months (unopened) and anywhere between 3 to 6 months after the container is open. This shelf life is substantially longer than tested storage periods demonstrated in ePADs which varies from 1 week to 2 months.<sup>48, 50, 149</sup> Most of these ePADs are reported to retain >90% activity within 10 to 30 days storage at 4°C or -20°C.<sup>40, 49, 74, 118, 149, 153</sup> Room temperature (RT) storage leads to faster degradation especially on highly modified electrodes,<sup>149</sup> while bare

electrodes can last longer at RT.<sup>150</sup> Up to 60 days stability over storage was reported by Sun and coworkers on their MIP-based device,<sup>48</sup> showing superior stability of this type of affinity sensor over the antibody-based ones.<sup>50, 74</sup> It is apparent that more studies are needed to investigate the inherent stability of sensor components within ePADs and optimize the fabrication as well as storage condition to achieve acceptable shelf life for commercialization. There have been multiple studies reported on improving stability of protein on electrodes<sup>202-204</sup> and on paper substrate.<sup>205</sup> More of this type of investigation is anticipated as the field continues to grow to meet the practical needs.

### **Multiplexing ability**

Another aspect of paper-based sensors that garners interest, especially for POCT application, is ability to perform multiplexed detection. Simultaneous determination of glucose, uric acid and lactate has been reported in early ePADs with detection limits ranging from 0.1 to 1.8 mM.<sup>8, 87</sup> These ePADs have separate electrode sets that were modified with enzymes necessary for detection of each analyte. Similar strategy is commonly applied in multiplexed paper-based immunosensors where each electrode is modified with recognition element for each target analyte.<sup>136, 137, 206</sup> Multiplexed detection of metal ions is often achieved using single electrode setup as long as the redox potential for each analyte does not significantly overlap with one another.<sup>28, 175</sup> While multiplexing arguably improves efficiency of the analysis, operation for such device should be kept simple and straightforward to avoid user error as much as possible. One possible way to achieve this is by engineering device operation to simplify the flow process of the assay.<sup>137</sup> Another way is to design data processing software that can extract information from measured electrochemical signals and display them in a more user-friendly fashion.

## **7. Summary and Future Outlook**

When constructing an ePAD, many factors are taken into consideration including cost, ease of fabrication, desired analytical performance and viability for field/POC applications. Carbon composite electrodes are often employed in ePADs due to their affordability. However, these electrodes often lack in electrochemical performance compared to conventional metallic electrodes. Moving forward, studies on improving the electrochemical properties of the inks used in these techniques are still necessary through altering the composition and utilization of catalysts.

Employing new electrode materials such as the TPEs and reevaluating electrode geometry may also improve detection in ePADs. To improve performance of the devices such as shorter analysis time, precise control of multistep assays and ability for multiplexed detection, multilayer geometry has been implemented in recent ePADs. More studies and engineering of such devices are still expected to allow for device automation and simplify assay operation for non-trained users of ePADs in the field or at POC.

The overall trends in sensing motifs used in ePADs are aimed at decreasing assay complexity for users, improving device longevity, and lowering limits of detection. From the simplest motif such as direct detection to the more complex affinity and electrochemiluminescence assays, nanomaterials incorporated into electrodes are reducing fouling, increasing surface area and improving selectivity and sensitivity in ePADs. These trends will likely continue, and new nanomaterials will be incorporated for enhanced detection and the paper substrate will continue to be used to automate assay steps for the various detection motifs and make the devices more user friendly. For direct detection of redox active metals and small molecules, improving working electrode materials for higher sensitivity, lower detection limits, and better peak separation for simultaneous detection will continue to be a focus. Potentiometric detection will be geared toward simplifying platforms for new ion detection, multiple analyte determination, and expanding ISE detection to field and POC use. New enzymatic ePADs could focus on improving electrode materials and enzyme storage stability, however, nanomaterials may increasingly be used to replace some of the functions of enzymes in ePADs. For electrochemical affinity ePADs, there is a push toward label-free detection over other affinity detection methods and this trend will likely continue. Along with more traditional recognition elements such as antibodies and nucleic acids, less conventional recognition elements such as MIPs and whole cells will increasingly be incorporated into ePADs to provide greater versatility and stability. Electrochemiluminescence detection will still be useful for its high signal to noise for trace detection in complex matrices.

While most of measurements using ePADs were still performed using quite expensive bench-top instruments, significant efforts have been made toward creating affordable portable potentiostats that can perform electrochemical measurements beyond what typical glucometer does. More collaborative work on testing and deploying these portable instruments for various field and POC applications are still required to bring these

prototyped instruments into wider use. The use of printed electronics is also potential to create customized all-in-one ePADs that are both user-friendly and highly portable.<sup>207</sup> Performing field evaluation of the laboratory-developed ePADs is greatly of importance, yet still challenging to do. Lack of information on how these ePADs will perform in the real world is one of the barriers to finding industrial partners for commercialization. Multidisciplinary collaborations to conduct field evaluation of these ePADs should be a part of research focus since information generated from this study will be very valuable for designing practical sensing devices. Last but not least, improving stability of current ePADs should also be another focus of the field moving forward.

### Conflict of interest

Authors declared no conflict of interest

### Acknowledgement

The authors thank the National Science Foundation (CHE1710222), the National Institutes of Health (ES024719), and the Center for Disease Control (OH010662) for financial support.

### References

1. G. S. Walpole, *Biochem. J.*, 1913, **7**, 260-267.
2. R. Conden, *Nature*, 1948, **162**, 359-361.
3. J. Hu, S. Q. Wang, L. Wang, F. Li, B. Pingguan-Murphy, T. J. Lu and F. Xu, *Biosens. Bioelectron.*, 2014, **54**, 585-597.
4. A. W. Martinez, S. T. Phillips, M. J. Butte and G. M. Whitesides, *Angew. Chem. Int.*, 2007, **46**, 1318-1320.
5. D. M. Cate, J. A. Adkins, J. Mettakoonpitak and C. S. Henry, *Anal. Chem.*, 2015, **87**, 19-41.
6. K. Yamada, H. Shibata, K. Suzuki and D. Citterio, *Lab Chip*, 2017, **17**, 1206-1249.
7. G. G. Morbioli, T. Mazzu-Nascimento, A. M. Stockton and E. Carrilho, *Anal. Chim. Acta*, 2017, **970**, 1-22.
8. W. Dungchai, O. Chailapakul and C. S. Henry, *Anal. Chem.*, 2009, **81**, 5821-5826.
9. J. Adkins, K. Boehle and C. Henry, *Electrophoresis*, 2015, **36**, 1811-1824.
10. W. J. Paschoalino, S. Kogikoski Jr, J. T. Barragan, J. F. Giarola, L. Cantelli, T. M. Rabelo, T. M. Pessanha and L. T. Kubota, *ChemElectroChem*, 2019, **6**, 10-30.
11. Y. He, Y. Wu, J.-Z. Fu and W.-B. Wu, *RSC Adv.*, 2015, **5**, 78109-78127.
12. V. B. C. Lee, N. F. Mom-Mum, E. Tamiya and M. U. Ahmed, *Anal. Sci.*, 2018, **34**, 7-18.
13. R. H. Müller and D. L. Clegg, *Anal. Chem.*, 1949, **21**, 1123-1125.
14. W. Dungchai, O. Chailapakul and C. S. Henry, *Analyst*, 2011, **136**, 77-82.

15. E. Carrilho, A. W. Martinez and G. M. Whitesides, *Anal. Chem.*, 2009, **81**, 7091-7095.
16. O. Amor-Gutierrez, E. Costa-Rama and M. T. Fernandez-Abedul, *Biosens. Bioelectron.*, 2019, **135**, 64-70.
17. S. Nantaphol, A. A. Kava, R. B. Channon, T. Kondo, W. Siangproh, O. Chailapakul and C. S. Henry, *Anal. Chim. Acta*, 2019, **1056**, 88-95.
18. A. Sanchez-Calvo, M. T. Fernandez-Abedul, M. C. Blanco-Lopez and A. Costa-Garcia, *Sens. Actuators B-Chem.*, 2019, **290**, 87-92.
19. S. Chaiyo, E. Mehmeti, W. Siangproh, T. L. Hoang, H. P. Nguyen, O. Chailapakul and K. Kalcher, *Biosens. Bioelectron.*, 2018, **102**, 113-120.
20. S. Cinti, L. Fiore, R. Massoud, C. Cortese, D. Moscone, G. Palleschi and F. Arduini, *Talanta*, 2018, **179**, 186-192.
21. C. M. Moreira, S. V. Pereira, J. Raba, F. A. Bertolino and G. A. Messina, *Clin. Chim. Acta*, 2018, **486**, 59-65.
22. P. I. Nanni, A. Gonzalez-Lopez, E. Nunez-Bajo, R. E. Madrid and M. T. Fernandez-Abedul, *ChemElectroChem*, 2018, **5**, 4036-4045.
23. Y. Panraksa, W. Siangproh, T. Khampieng, O. Chailapakul and A. Apilux, *Talanta*, 2018, **178**, 1017-1023.
24. G. Scordo, D. Moscone, G. Palleschi and F. Arduini, *Sens. Actuators B: Chem.*, 2018, **258**, 1015-1021.
25. P. Teengam, W. Siangproh, A. Tuantranont, T. Vilaivan, O. Chailapakul and C. S. Henry, *Anal. Chim. Acta*, 2018, **1044**, 102-109.
26. V. K. Tran, E. Ko, Y. F. Geng, M. K. Kim, G. H. Jin, S. E. Son, W. Hur and G. H. Seong, *J. Electroanal. Chem.*, 2018, **826**, 29-37.
27. M. N. Tsaloglou, A. Nemiroski, G. Camci-Unal, D. C. Christodouleas, L. P. Murray, J. T. Connelly and G. M. Whitesides, *Anal. Biochem.*, 2018, **543**, 116-121.
28. C. Kokkinos, A. Economou and D. Giokas, *Sens. Actuators B: Chem.*, 2018, **260**, 223-226.
29. T. R. de Oliveira, W. T. Fonseca, G. D. Setti and R. C. Faria, *Talanta*, 2019, **195**, 480-489.
30. H. C. Qin, Z. Y. Zhu, W. L. Ji and M. N. Zhang, *Electroanalysis*, 2018, **30**, 1022-1027.
31. J. Zhang, Z. Yang, Q. Liu and H. Liang, *Talanta*, 2019, **202**, 384-391.
32. M. Amatatongchai, J. Sitanurak, W. Sroysee, S. Sodanath, S. Chairam, P. Jarujamrus, D. Nacapricha and P. A. Lieberzeit, *Anal. Chim. Acta*, 2019, **1077**, 255-265.
33. N. Dossi, R. Toniolo, F. Terzi, N. Sdrigotti, F. Tubaro and G. Bontempelli, *Anal. Chim. Acta*, 2018, **1040**, 74-80.
34. E. M. Fenton, M. R. Mascarenas, G. P. López and S. S. Sibbett, *ACS Appl. Mater. Interfaces*, 2009, **1**, 124-129.
35. E. L. Fava, T. A. Silva, T. M. de Prado, F. C. de Moraes, R. C. Faria and O. Fatibello-Filho, *Talanta*, 2019, **203**, 280-286.
36. F. H. Cincotto, E. L. Fava, F. C. Moraes, O. Fatibello-Filho and R. C. Faria, *Talanta*, 2019, **195**, 62-68.
37. V. Primpray, O. Chailapakul, M. Tokeshi, T. Rojanarata and W. Laiwattanapaisal, *Anal. Chim. Acta*, 2019, **1078**, 16-23.
38. F. J. V. Gomez, P. A. Reed, D. G. Casamachin, J. R. de la Rosa, G. Chumanov, M. F. Silva and C. D. Garcia, *Anal. Methods*, 2018, **10**, 4020-4027.
39. Y. Wang, J. Luo, J. Liu, X. Li, Z. Kong, H. Jin and X. Cai, *Biosens. Bioelectron.*, 2018, **107**, 47-53.
40. X. Sun, H. Wang, Y. Jian, F. Lan, L. Zhang, H. Liu, S. Ge and J. Yu, *Biosens. Bioelectron.*, 2018, **105**, 218-225.
41. K. Pungjunun, S. Chaiyo, I. Jantrahong, S. Nantaphol, W. Siangproh and O. Chailapakul, *Microchim. Acta*, 2018, **185**, 324.

42. R. B. Channon, M. P. Nguyen, A. G. Scorzelli, E. M. Henry, J. Volckens, D. S. Dandy and C. S. Henry, *Lab Chip*, 2018, **18**, 793-802.
43. E. Elizalde, R. Urteaga and C. L. Berli, *Lab Chip*, 2015, **15**, 2173-2180.
44. A. W. Martinez, S. T. Phillips and G. M. Whitesides, *Proc. Natl. Acad. Sci.*, 2008, **105**, 19606-19611.
45. Y. Wang, J. P. Luo, J. T. Liu, S. Sun, Y. Xiong, Y. Y. Ma, S. Yan, Y. Yang, H. B. Yin and X. X. Cai, *Biosens. Bioelectron.*, 2019, **136**, 84-90.
46. Q. Cao, B. Liang, T. Tu, J. Wei, L. Fang and X. Ye, *RSC Adv.*, 2019, **9**, 5674-5681.
47. Y. Z. Huang, L. Li, Y. Zhang, L. N. Zhang, S. G. Ge and J. H. Yu, *Biosens. Bioelectron.*, 2019, **126**, 339-345.
48. X. Sun, Y. Jian, H. Wang, S. Ge, M. Yan and J. Yu, *ACS Appl. Mater. Interfaces*, 2019, **11**, 16198-16206.
49. S. Boonkaew, S. Chaiyo, S. Jampasa, S. Rengpipat, W. Siangproh and O. Chailapakul, *Microchim. Acta*, 2019, **186**, 153.
50. Y. Boonyasit, O. Chailapakul and W. Laiwattanapaisal, *Biosens. Bioelectron.*, 2019, **130**, 389-396.
51. N. Colozza, K. Kehe, G. Dionisi, T. Popp, A. Tsoutsoulopoulos, D. Steinritz, D. Moscone and F. Arduini, *Biosens. Bioelectron.*, 2019, **129**, 15-23.
52. S. G. Ge, J. G. Zhao, S. P. Wang, F. F. Lan, M. Yan and J. H. Yu, *Biosens. Bioelectron.*, 2018, **102**, 411-417.
53. J. Xu, Y. Zhang, L. Li, Q. Kong, L. Zhang, S. Ge and J. Yu, *ACS Appl. Mater. Interfaces*, 2018, **10**, 3431-3440.
54. H. Wang, C. Zhou, X. Sun, Y. Jian, Q. Kong, K. Cui, S. Ge and J. Yu, *Biosens. and Bioelectron.*, 2018, **117**, 651-658.
55. F. Arduini, S. Cinti, V. Caratelli, L. Amendola, G. Palleschi and D. Moscone, *Biosens. and Bioelectron.*, 2019, **126**, 346-354.
56. V. Soum, S. Park, A. I. Brilian, O. S. Kwon and K. Shin, *Micromachines*, 2019, **10**, 516.
57. E. Noviana, K. J. Klunder, R. B. Channon and C. S. Henry, *Anal. Chem.*, 2019, **91**, 2431-2438.
58. S. Devarakonda, R. Singh, J. Bhardwaj and J. Jang, *Sensors*, 2017, **17**, 2597.
59. S. Nantaphol, R. B. Channon, T. Kondo, W. Siangproh, O. Chailapakul and C. S. Henry, *Anal. Chem.*, 2017, **89**, 4100-4107.
60. S. Cinti, N. Colozza, I. Cacciotti, D. Moscone, M. Polomoshnov, E. Sowade, R. R. Baumann and F. Arduini, *Sens. Actuators B: Chem.*, 2018, **265**, 155-160.
61. W. Kit-Anan, A. Olarnwanich, C. Sriprachuabwong, C. Karuwan, A. Tuantranont, A. Wisitsoraat, W. Srituravanich and A. Pimpin, *J. Electroanal. Chem.*, 2012, **685**, 72-78.
62. N. Ruecha, O. Chailapakul, K. Suzuki and D. Citterio, *Anal. Chem.*, 2017, **89**, 10608-10616.
63. R. P. Tortorich, H. Shamkhalichenar and J. W. Choi, *Appl. Sci.*, 2018, **8**, 288.
64. H. Shamkhalichenar and J. W. Choi, *J. Electrochem. Soc.*, 2017, **164**, B3101-B3106.
65. T. H. da Costa, E. Song, R. P. Tortorich and J. W. Choi, *ECS J. Solid State Sci. Technol.*, 2015, **4**, S3044-S3047.
66. R. B. Channon, Y. Yang, K. M. Feibelman, B. J. Geiss, D. S. Dandy and C. S. Henry, *Anal. Chem.*, 2018, **90**, 7777-7783.
67. W. R. de Araujo, C. M. Frasson, W. A. Ameku, J. R. Silva, L. Angnes and T. R. Paixão, *Angew. Chem. Int.*, 2017, **56**, 15113-15117.
68. A. A. Dias, T. M. G. Cardoso, C. L. S. Chagas, V. X. G. Oliveira, R. A. A. Munoz, C. S. Henry, M. H. P. Santana, T. Paixao and W. K. T. Coltro, *Electroanalysis*, 2018, **30**, 2250-2257.
69. V. X. G. Oliveira, A. A. Dias, L. L. Carvalho, T. M. G. Cardoso, F. Colmati and W. K. T. Coltro, *Anal. Sci.*, 2018, **34**, 91-95.

70. R. F. Carvalhal, M. S. Kfourit, M. H. d. O. Piazzetta, A. L. Gobbi and L. T. Kubota, *Anal. Chem.*, 2010, **82**, 1162-1165.
71. M. Parrilla, R. Canovas and F. J. Andrade, *Biosens. Bioelectron.*, 2017, **90**, 110-116.
72. E. Núñez-Bajo, M. C. Blanco-López, A. Costa-García and M. T. Fernández-Abedul, *Talanta*, 2018, **178**, 160-165.
73. F. Darain, S. U. Park and Y. B. Shim, *Biosens. Bioelectron.*, 2003, **18**, 773-780.
74. N. Ruecha, K. Shin, O. Chailapakul and N. Rodthongkum, *Sens. Actuators B: Chem.*, 2019, **279**, 298-304.
75. S. Nantaphol, W. Jesadabundit, O. Chailapakul and W. Siangproh, *J. Electroanal. Chem.*, 2019, **832**, 480-485.
76. M. Pavithra, S. Muruganand and C. Parthiban, *Sens. Actuators B: Chem.*, 2018, **257**, 496-503.
77. M. Li, Y. T. Li, D. W. Li and Y. T. Long, *Anal. Chim. Acta*, 2012, **734**, 31-44.
78. R. L. McCreery, *Chem. Rev.*, 2008, **108**, 2646-2687.
79. N. Dossi, R. Toniolo, A. Pizzariello, F. Impellizzieri, E. Piccin and G. Bontempelli, *Electrophoresis*, 2013, **34**, 2085-2091.
80. Z. Li, F. Li, Y. Xing, Z. Liu, M. You, Y. Li, T. Wen, Z. Qu, X. L. Li and F. Xu, *Biosens. Bioelectron.*, 2017, **98**, 478-485.
81. S. E. Fosdick, M. J. Anderson, C. Renault, P. R. DeGregory, J. A. Loussaert and R. M. Crooks, *Anal. Chem.*, 2014, **86**, 3659-3666.
82. J. A. Adkins and C. S. Henry, *Anal. Chim. Acta*, 2015, **891**, 247-254.
83. J. G. Giuliani, T. E. Benavidez, G. M. Duran, E. Vinogradova, A. Rios and C. D. Garcia, *J. Electroanal. Chem.*, 2016, **765**, 8-15.
84. M. Santhiago, C. S. Henry and L. T. Kubota, *Electrochim. Acta*, 2014, **130**, 771-777.
85. K. J. Klunder, Z. Nilsson, J. B. Sambur and C. S. Henry, *J. Am. Chem. Soc.*, 2017, **139**, 12623-12631.
86. S. Yamamoto and S. Uno, *Sensors*, 2018, **18**, 730.
87. C. Zhao, M. M. Thuo and X. Liu, *Sci. Technol. Adv. Mater.*, 2013, **14**, 54402-54402.
88. J. Wang and M. Musameh, *Anal. Chem.*, 2003, **75**, 2075-2079.
89. F. Céspedes, E. Martínez-Fàbregas and S. Alegret, *Anal. Chim. Acta*, 1993, **284**, 21-26.
90. J. M. Petroni, B. G. Lucca, L. C. da Silva, D. C. B. Alves and V. S. Ferreira, *Electroanalysis*, 2017, **29**, 2628-2637.
91. N. Nontawong, M. Amatatongchai, W. Wuepchaiyaphum, S. Chairam, S. Pimmongkol, S. Panich, S. Tamuang and P. Jarujamrus, *Int. J. Electrochem. Sci.*, 2018, **13**, 6940-6957.
92. P. Wang, M. Y. Wang, F. Y. Zhou, G. H. Yang, L. L. Qu and X. M. Miao, *Electrochem. Commun.*, 2017, **81**, 74-78.
93. J. Narang, C. Singhal, M. Khanuja, A. Mathur, A. Jain and C. S. Pundir, *Artif. Cells, Nanomed., Biotechnol.*, 2018, **46**, 1586-1593.
94. Z. H. Nie, C. A. Nijhuis, J. L. Gong, X. Chen, A. Kumachev, A. W. Martinez, M. Narovlyansky and G. M. Whitesides, *Lab Chip*, 2010, **10**, 477-483.
95. J. J. Shi, F. Tang, H. L. Xing, H. X. Zheng, L. H. Bi and W. Wang, *J. Braz. Chem. Soc.*, 2012, **23**, 1124-1130.
96. Q. M. Feng, Q. Zhang, C. G. Shi, J. J. Xu, N. Bao and H. Y. Gu, *Talanta*, 2013, **115**, 235-240.
97. S. N. Tan, L. Y. Ge and W. Wang, *Anal. Chem.*, 2010, **82**, 8844-8847.
98. G. V. Martins, A. C. Marques, E. Fortunato and M. G. F. Sales, *Electrochim. Acta*, 2018, **284**, 60-68.
99. S. M. Armas, A. J. Manhan, O. Younce, P. Calvo-Marzal and K. Y. Chumbimuni-Torres, *Sens. Actuator B-Chem.*, 2018, **255**, 1781-1787.

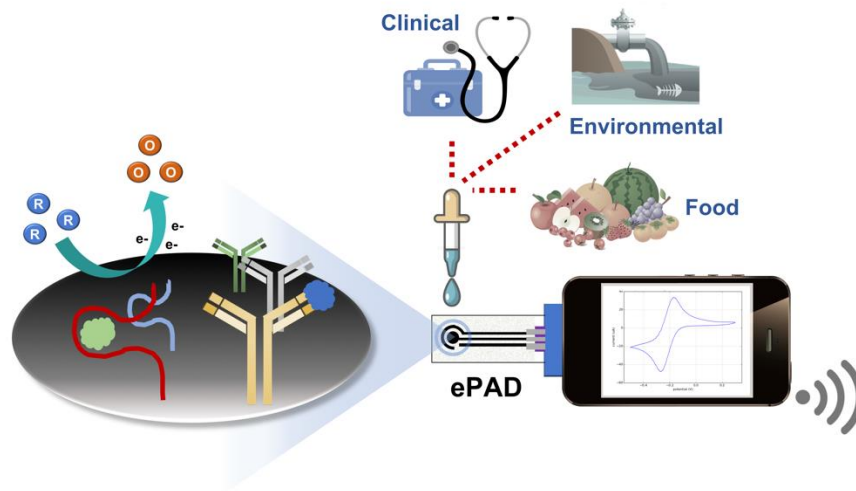
100. J. G. Bell, M. P. S. Mousavi, M. K. Abd El-Rahmana, E. K. W. Tan, S. Homer-Vanniasinkam and G. M. Whitesides, *Biosens. Bioelectron.*, 2019, **126**, 115-121.
101. S. T. Mensah, Y. Gonzalez, P. Calvo-Marzal and K. Y. Chumbimuni-Torres, *Anal. Chem.*, 2014, **86**, 7269-7273.
102. G. Scordo, D. Moscone, G. Palleschi and F. Arduini, *Sens. Actuator B-Chem.*, 2018, **258**, 1015-1021.
103. S. Cinti, C. Minotti, D. Moscone, G. Palleschi and F. Arduini, *Biosens. Bioelectron.*, 2017, **93**, 46-51.
104. G. Martinez-Garcia, E. Perez-Julian, L. Agui, N. Cabre, J. Joven, P. Yanez-Sedeno and J. M. Pingarron, *Biosensors*, 2017, **7**.
105. R. Pelton, *TrAC-Trends Anal. Chem.*, 2009, **28**, 925-942.
106. S. Cinti, M. Basso, D. Moscone and F. Arduini, *Anal. Chim. Acta*, 2017, **960**, 123-130.
107. O. Amor-Gutierrez, E. C. Rama, A. Costa-Garcia and M. T. Fernandez-Abedul, *Biosens. Bioelectron.*, 2017, **93**, 40-45.
108. O. Amor-Gutierrez, E. C. Rama, M. T. Fernandez-Abedul and A. Costa-Garcia, *J. Chem. Edu.*, 2017, **94**, 806-812.
109. X. X. Zheng, L. Li, K. Cui, Y. Zhang, L. N. Zhang, S. G. Ge and J. H. Yu, *ACS Appl. Mater. Interfaces*, 2018, **10**, 3333-3340.
110. B. Wei, K. Mao, N. Liu, M. Zhang and Z. Yang, *Biosens. Bioelectron.*, 2018, **121**, 41-46.
111. J. Mettakoonpitak, K. Boehle, S. Nantaphol, P. Teengam, J. A. Adkins, M. Srisa-Art and C. S. Henry, *Electroanalysis*, 2016, **28**, 1420-1436.
112. Z. Z. Yu, Y. Tang, G. N. Cai, R. R. Ren and D. P. Tang, *Anal. Chem.*, 2019, **91**, 1222-1226.
113. J. A. Adkins, E. Noviana and C. S. Henry, *Anal. Chem.*, 2016, **88**, 10639-10647.
114. M. L. Scala-Benuzzi, J. Raba, G. Soler-Illia, R. J. Schneider and G. A. Messina, *Anal. Chem.*, 2018, **90**, 4104-4111.
115. P. Teengam, W. Siangproh, A. Tuantranont, C. S. Henry, T. Vilaivan and O. Chailapakul, *Anal. Chim. Acta*, 2017, **952**, 32-40.
116. S. Cinti, E. Proietti, F. Casotto, D. Moscone and F. Arduini, *Anal. Chem.*, 2018, **90**, 13680-13686.
117. B. C. Zhu and J. Travas-Sejdic, *Analyst*, 2018, **143**, 687-694.
118. C. T. Kokkinos, D. L. Giokas, A. S. Economou, P. S. Petrou and S. E. Kakabakos, *Anal. Chem.*, 2018, **90**, 1092-1097.
119. A. H. Kamel, X. J. Jiang, P. J. Li and R. N. Liang, *Anal. Methods*, 2018, **10**, 3890-3895.
120. J. Qi, B. Li, Na Zhou, X. Wang, D. Deng, L. Luo, and L. Chen, *Biosens. Bioelectron.*, 2019, **142**, 111533.
121. D. Jiang, P. Ge, L. Wang, H. Jiang, M. Yang, L. Yuan, Q. Ge, W. Fang and X. Ju, *Biosens. Bioelectron.*, 2019, **130**, 299-306.
122. R. J. Gui, H. Jin, H. J. Guo and Z. H. Wang, *Biosens. Bioelectron.*, 2018, **100**, 56-70.
123. Y. Chen, J. Wang, Z. M. Liu, X. G. Wang, X. Li and G. Q. Shan, *Biochem. Eng. J.*, 2018, **129**, 1-6.
124. J. L. Delaney, C. F. Hogan, J. F. Tian and W. Shen, *Anal. Chem.*, 2011, **83**, 1300-1306.
125. M. M. Richter, *Chem. Rev.*, 2004, **104**, 3003-3036.
126. E. Sciuto, M. Santangelo, G. Villaggio, F. Sinatra, C. Bongiorno, G. Nicotra and S. Libertino, *Sens. Biosensing Res.*, 2015, **6**, 67-71.
127. X. Zhou, D. Zhu, Y. Liao, W. Liu, H. Liu, Z. Ma and D. Xing, *Nat. Protoc.*, 2014, **9**, 1146-1159.
128. N. Sardesai, S. Pan and J. Rusling, *Chem. Commun.*, 2009, 4968-4970.
129. Z. Deng, O. Schulz, S. Lin, B. Ding, X. Liu, X. Wei, R. Ros, H. Yan and Y. Liu, *J. Am. Chem. Soc.*, 2010, **132**, 5592-5593.
130. H. Zhu, X. Wang, Y. Li, Z. Wang, F. Yang and X. Yang, *Chem. Commun.*, 2009, 5118-5120.

131. D. Lin, J. Wu, F. Yan, S. Deng and H. Ju, *Anal. Chem.*, 2011, **83**, 5214-5221.
132. Y. Shan, J. J. Xu and H. Y. Chen, *Nanoscale*, 2011, **3**, 2916-2923.
133. X. Jiang, Y. Chai, H. Wang and R. Yuan, *Biosens. Bioelectron.*, 2014, **54**, 20-26.
134. L. D. Wu, C. Ma, L. Ge, Q. K. Kong, M. Yan, S. G. Ge and J. H. Yu, *Biosens. Bioelectron.*, 2015, **63**, 450-457.
135. S. R. Chinnadayala, J. Park, H. T. N. Le, M. Santhosh, A. N. Kadam and S. Cho, *Biosens. Bioelectron.*, 2019, **126**, 68-81.
136. L. Ge, J. Yan, X. Song, M. Yan, S. Ge and J. Yu, *Biomaterials*, 2012, **33**, 1024-1031.
137. X. Sun, B. Li, C. Tian, F. Yu, N. Zhou, Y. Zhan and L. Chen, *Anal. Chim. Acta*, 2018, **1007**, 33-39.
138. C. M. Gao, M. Su, Y. H. Wang, S. G. Ge and J. H. Yu, *RSC Adv.*, 2015, **5**, 28324-28331.
139. J. X. Yan, M. Yan, L. Ge, J. H. Yu, S. G. Ge and J. D. Huang, *Chem. Commun.*, 2013, **49**, 1383-1385.
140. Q. M. Feng, J. B. Pan, H. R. Zhang, J. J. Xu and H. Y. Chen, *Chem. Commun.*, 2014, **50**, 10949-10951.
141. D. Wang, C. L. Liu, Y. Liang, Y. Su, Q. P. Shang and C. S. Zhang, *J. Electrochem. Soc.*, 2018, **165**, B361-B369.
142. F. Mavr e, R. K. Anand, D. R. Laws, K. F. Chow, B. Y. Chang, J. A. Crooks and R. M. Crooks, *Anal. Chem.*, 2010, **82**, 8766-8774.
143. K. N. Knust, E. Sheridan, R. K. Anand and R. M. Crooks, *Lab Chip*, 2012, **12**, 4107-4114.
144. X. Zhang, N. Bao, X. Luo and S. N. Ding, *Biosens. Bioelectron.*, 2018, **114**, 44-51.
145. H. M. Yang, Y. Zhang, L. Li, L. N. Zhang, F. F. Lan and J. H. Yu, *Anal. Chem.*, 2017, **89**, 7511-7519.
146. M. P. Nguyen, N. A. Meredith, S. P. Kelly and C. S. Henry, *Anal. Chim. Acta*, 2018, **1017**, 20-25.
147. M. Zhang, L. Ge, S. G. Ge, M. Yan, J. H. Yu, J. D. Huang and S. Liu, *Biosens. Bioelectron.*, 2013, **41**, 544-550.
148. S. Wang, L. Ge, Y. Zhang, X. Song, N. Li, S. Ge and J. Yu, *Lab Chip*, 2012, **12**, 4489-4498.
149. H. Wang, Y. Jian, Q. Kong, H. Liu, F. Lan, L. Liang, S. Ge and J. Yu, *Sens. Actuators B: Chem.*, 2018, **257**, 561-569.
150. P. Wang, Z. Cheng, Q. Chen, L. Qu, X. Miao and Q. Feng, *Sens. Actuators B: Chem.*, 2018, **256**, 931-937.
151. J. Chouler,  . Cruz-Izquierdo, S. Rengaraj, J. L. Scott and M. Di Lorenzo, *Biosens. Bioelectron.*, 2018, **102**, 49-56.
152. P. J. Lamas-Ardisana, G. Mart nez-Paredes, L. A norga and H. J. Grande, *Biosens. Bioelectron.*, 2018, **109**, 8-12.
153. L. Fan, Q. Hao and X. Kan, *Sens. Actuators B: Chem.*, 2018, **256**, 520-527.
154. G. V. Research, Paper Diagnostics Market Analysis Report By Device Type (Diagnostics, Monitoring), By Application, By Product (Lateral Flow Assays, Paper Based Microfluidics), By End Use, and Segment Forecasts, 2018 - 2025, <https://www.grandviewresearch.com/industry-analysis/paper-diagnostics-market>, (accessed July 14, 2019).
155. E. B. Bahadır and M. K. Sezgent rk, *TrAC-Trends Anal. Chem.*, 2016, **82**, 286-306.
156. S. Clarke and J. Foster, *British J. Biomed. Sci.*, 2012, **69**, 83-93.
157. A. W. Martinez, S. T. Phillips, G. M. Whitesides and E. Carrilho, *Anal. Chem.*, 2010, **82**, 3-10.
158. L. Wang, W. Chen, D. Xu, B. S. Shim, Y. Zhu, F. Sun, L. Liu, C. Peng, Z. Jin and C. Xu, *Nano Lett.*, 2009, **9**, 4147-4152.
159. J. Lu, S. Ge, L. Ge, M. Yan and J. Yu, *Electrochim. Acta*, 2012, **80**, 334-341.
160. D. Zang, L. Ge, M. Yan, X. Song and J. Yu, *Chem. Commun.*, 2012, **48**, 4683-4685.
161. F. Y. Kong, S. X. Gu, W. W. Li, T. T. Chen, Q. Xu and W. Wang, *Biosens. Bioelectron.*, 2014, **56**, 77-82.

162. N. Ruecha, N. Rodthongkum, D. M. Cate, J. Volckens, O. Chailapakul and C. S. Henry, *Anal. Chim. Acta*, 2015, **874**, 40-48.
163. EPA, National Primary Drinking Water Regulations, <https://www.epa.gov/ground-water-and-drinking-water/national-primary-drinking-water-regulations>, (accessed July 15, 2019).
164. A. Abbaspour, F. Norouz-Sarvestani, A. Noori and N. Soltani, *Biosens. Bioelectron.*, 2015, **68**, 149-155.
165. J. Bhardwaj, S. Devarakonda, S. Kumar and J. Jang, *Sens. Actuators B: Chem.*, 2017, **253**, 115-123.
166. E. Fu, B. Lutz, P. Kauffman and P. Yager, *Lab Chip*, 2010, **10**, 918-920.
167. B. R. Lutz, P. Trinh, C. Ball, E. Fu and P. Yager, *Lab Chip*, 2011, **11**, 4274-4278.
168. A. Apilux, Y. Ukita, M. Chikae, O. Chailapakul and Y. Takamura, *Lab Chip*, 2013, **13**, 126-135.
169. A. Abbas, A. Brimer, J. M. Slocik, L. Tian, R. R. Naik and S. Singamaneni, *Anal. Chem.*, 2013, **85**, 3977-3983.
170. S. H. Yeh, K. H. Chou and R. J. Yang, *Lab Chip*, 2016, **16**, 925-931.
171. B. Y. Moghadam, K. T. Connelly and J. D. Posner, *Anal. Chem.*, 2014, **86**, 5829-5837.
172. H. Liu, Y. Xiang, Y. Lu and R. M. Crooks, *Angew. Chem. Int.*, 2012, **51**, 6925-6928.
173. L. Ge, S. Wang, J. Yu, N. Li, S. Ge and M. Yan, *Adv. Funct. Mater.*, 2013, **23**, 3115-3123.
174. M. Fang, L. Zhou, H. Zhang, L. Liu and Z.-Y. Gong, *Food Chem.*, 2019, **274**, 156-161.
175. J. Mettakoonpitak, J. Mehaffy, J. Volckens and C. S. Henry, *Electroanalysis*, 2017, **29**, 880-889.
176. J. Riu and F. X. Rius, *Anal. Chem.*, 1996, **68**, 1851-1857.
177. A. G. González and M. Á. Herrador, *TrAC-Trends Anal. Chem.*, 2007, **26**, 227-238.
178. S. Chaiyo, A. Apiluk, W. Siangproh and O. Chailapakul, *Sens. Actuators B: Chem.*, 2016, **233**, 540-549.
179. USFDA, Self Monitoring Blood Glucose Test System for Over-the-Counter Use, <https://www.fda.gov/media/119828/download>, (accessed July 17, 2019).
180. A. K. Yetisen, M. S. Akram and C. R. Lowe, *Lab Chip*, 2013, **13**, 2210-2251.
181. J. Wang, M. R. N. Monton, X. Zhang, C. D. Filipe, R. Pelton and J. D. Brennan, *Lab Chip*, 2014, **14**, 691-695.
182. V. Rajendra, C. Sicard, J. D. Brennan and M. A. Brook, *Analyst*, 2014, **139**, 6361-6365.
183. M. Sophocleous and J. K. Atkinson, *Sens. Actuators A: Phys.*, 2017, **267**, 106-120.
184. H. Brisset, J. F. Briand, R. Barry-Martinet, T. H. Duong, P. Frère, F. Gohier, P. Leriche and C. Bressy, *Anal. Chem.*, 2018, **90**, 4978-4981.
185. L. Barhoumi, F. G. Bellagambi, F. M. Vivaldi, A. Baraket, Y. Clément, N. Zine, M. Ben Ali, A. Elaissari and A. Errachid, *Sensors*, 2019, **19**, 692.
186. N. Komuro, S. Takaki, K. Suzuki and D. Citterio, *Anal. Bioanal. Chem.*, 2013, **405**, 5785-5805.
187. K. Yamada, T. G. Henares, K. Suzuki and D. Citterio, *Angew. Chem. Int.*, 2015, **54**, 5294-5310.
188. H. Liu and R. M. Crooks, *J. Am. Chem. Soc.*, 2011, **133**, 17564-17566.
189. S. G. Jeong, S. H. Lee, C. H. Choi, J. Kim and C. S. Lee, *Lab Chip*, 2015, **15**, 1188-1194.
190. Z. Nie, F. Deiss, X. Liu, O. Akbulut and G. M. Whitesides, *Lab Chip*, 2010, **10**, 3163-3169.
191. C. C. Wang, J. W. Hennek, A. Ainla, A. A. Kumar, W. J. Lan, J. Im, B. S. Smith, M. Zhao and G. M. Whitesides, *Anal. Chem.*, 2016, **88**, 6326-6333.
192. Commercial Portable Potentiostats, <https://www.palmsens.com/potentiostat/portable-potentiostat>, <https://www.metrohm.com/en-gb/products-overview/electrochemistry/portable-potentiostats>, [http://www.dropsens.com/en/potentiostats\\_pag.html](http://www.dropsens.com/en/potentiostats_pag.html), (accessed July 18, 2019).
193. A. A. Rowe, A. J. Bonham, R. J. White, M. P. Zimmer, R. J. Yadgar, T. M. Hobza, J. W. Honea, I. Ben-Yaacov and K. W. Plaxco, *PloS One*, 2011, **6**, e23783.

194. A. Ainla, M. P. Mousavi, M.-N. Tsaloglou, J. Redston, J. G. Bell, M. T. Fernández-Abedul and G. M. Whitesides, *Anal. Chem.*, 2018, **90**, 6240-6246.
195. G. F. Giordano, M. B. Vicentini, R. C. Murer, F. Augusto, M. F. Ferrão, G. A. Helfer, A. B. da Costa, A. L. Gobbi, L. W. Hantao and R. S. Lima, *Electrochim. Acta*, 2016, **219**, 170-177.
196. A. Pal, H. E. Cuellar, R. Kuang, H. F. Caurin, D. Goswami and R. V. Martinez, *Adv. Mater. Technol.*, 2017, **2**, 1700130.
197. I. Ramfos, N. Vassiliadis, S. Blionas, K. Efstathiou, A. Fragoso, C. K. O'Sullivan and A. Birbas, *Biosens. Bioelectron.*, 2013, **47**, 482-489.
198. A. Nemiroski, D. C. Christodouleas, J. W. Hennek, A. A. Kumar, E. J. Maxwell, M. T. Fernández-Abedul and G. M. Whitesides, *Proc. Natl. Acad. Sci. USA*, 2014, **111**, 11984-11989.
199. M. D. Dryden and A. R. Wheeler, *PLoS One*, 2015, **10**, e0140349.
200. T. Dobbelaere, P. M. Vereecken and C. Detavernier, *HardwareX*, 2017, **2**, 34-49.
201. P. Lopin and K. V. Lopin, *PLoS One*, 2018, **13**, e0201353.
202. P. Asuri, S. S. Karajanagi, H. Yang, T. J. Yim, R. S. Kane and J. S. Dordick, *Langmuir*, 2006, **22**, 5833-5836.
203. J. Wang, J. Liu and G. Ceppra, *Anal. Chem.*, 1997, **69**, 3124-3127.
204. S. Rubenwolf, S. Kerzenmacher, R. Zengerle and F. von Stetten, *Appl. Microbiol. Biotechnol.*, 2011, **89**, 1315-1322.
205. E. W. Nery and L. T. Kubota, *J. Pharm. Biomed. Anal.* 2016, **117**, 551-559.
206. Y. Wu, P. Xue, Y. Kang and K. M. Hui, *Anal. Chem.*, 2013, **85**, 8661-8668.
207. V. Beni, D. Nilsson, P. Arven, P. Norberg, G. Gustafsson and A. P. Turner, *ECS J. Solid State Sci. Technol.*, 2015, **4**, S3001-S3005.

(Graphical abstract)



**Authors Bio:**

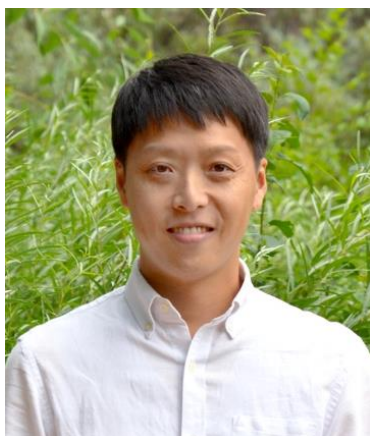
**Eka Noviana** obtained her B.S. in Pharmaceutical Science from Universitas Gadjah Mada, Indonesia, in 2012. She received her M.S. in Chemistry from the University of Arizona in 2015. She is currently a Ph.D. candidate at Colorado State University. Her research focuses on developing low-cost colorimetric and electrochemical sensors for bioanalytical applications.



**Cynthia P. McCord** received her B.S. in Chemistry from the University of West Florida in 2016. She is currently a 4<sup>th</sup> year analytical chemistry graduate student at Colorado State University. Her research focus is using thermoplastic carbon composite electrodes for electrochemical biosensing.



**Kaylee M. Clark** received her B.S. in Chemistry from Clemson University in 2017. Currently, she is a graduate student in the Chemistry Department at Colorado State University. Her current research is using thermoplastic electrodes to develop low-cost electrochemical devices for bioanalytical applications.



**Ilhoon Jang** received his Ph.D. in Mechanical Engineering from Hanyang University in 2018. He is currently a postdoctoral fellow in the Institute of Nano Science and Technology at Hanyang University, and a visiting researcher in the Chemistry Department at Colorado State University. His research focuses on flow control and modeling in paper-based analytical devices.



**Charles S. Henry** received his Ph.D. from the University of Arkansas followed by postdoctoral studies at the University of Kansas. He started his academic career at Mississippi State University before moving to Colorado State University in 2002, where he is currently Professor of Chemistry. His research interests lie broadly in the areas of microfluidics and electrochemistry with application to questions in bioanalytical and environmental chemistry.